UNIVERSITY OF LATVIA

Summary of Doctoral Thesis

Inga Pudža

IMPACT OF THE LOCAL STRUCTURE ON THE THERMOCHROMIC PROPERTIES OF COPPER MOLYBDATE AND ITS SOLID SOLUTIONSS

Riga 2022

UNIVERSITY OF LATVIA

FACULTY OF PHYSICS, MATHEMATICS AND OPTOMETRY

Inga Pudža

IMPACT OF THE LOCAL STRUCTURE ON THE THERMOCHROMIC PROPERTIES OF COPPER MOLYBDATE AND ITS SOLID SOLUTIONS

SUMMARY OF DOCTORAL THESIS

Submitted for the Doctoral degree in Physics and Astronomy
Subfield of Solid State Physics

Riga 2022

The doctoral thesis was carried out at the Institute of Solid State Physics of University of Latvia from 2017 to 2021.

The thesis contains the introduction, nine chapters, conclusions and thesis, reference list.

Form of thesis: dissertation in Physics and Astronomy, subfield of solid state physics.

Scientific supervisor:

Dr. phys. **Aleksejs Kuzmins**, senior researcher and the head of the EXAFS Spectroscopy Laboratory at Institute of Solid State Physics, University of Latvia.

Reviewers:

1) *Dr. phys.* **Anatolijs Šarakovskis**, University of Latvia;
2) *Dr. rer. nat.* **Wolfgang A. Caliebe**, Photon Science – Deutsches Elektronen-Synchrotron (DESY) (Germany);
3) Prof. *Ph.D.* **Anatoly I. Frenkel**, Stony Brook University (USA).

The thesis will be defended at the public session of Doctoral Committee of Physics, Astronomy and Mechanics, University of Latvia at 15:00 on May 11, 2022 in the conference hall of the Institute of Solid State Physics of University of Latvia.

The doctoral thesis and its summary are available at the Library of the University of Latvia (19 Raina Blvd, Riga) and Latvian Academic Library (10 Rupniecibas Str, Riga).

Chairman of the Doctoral Committee *Dr. phys.* **Anatolijs Šarakovskis**

Secretary of the Doctoral Committee **Agnese Ozoliņa**

ISBN 978-9934-18-821-3
ISBN 978-9934-18-822-0 (PDF)

Abstract

Copper molybdate ($CuMoO_4$) and related solid solutions are multifunctional materials exhibiting chromic properties, including thermochromism and piezochromism. Their colour change is caused by the lattice expansion/contraction, which affects the band gap, or a modification of the material structure upon a phase transition. Therefore, the knowledge of the structure and its temperature and composition dependence is crucial for understanding and controlling the functionality of these materials that determines their practical applications.

In this thesis, the structure-property relationships in $CuMoO_4$ and two series of solid solutions ($CuMo_{1-x}W_xO_4$ and $Cu_{1-x}Zn_xMoO_4$) were studied by X-ray absorption and resonant X-ray emission spectroscopies (XAS and RXES). The experimental results were supported by the reverse Monte-Carlo (RMC) simulations coupled with *ab initio* multiple-scattering calculations. The RXES method was used to determine changes in the local coordination of tungsten ions from the crystal field induced splitting of the 5d(W) states across the phase transitions in $CuMo_{1-x}W_xO_4$ solid solutions.

The obtained results enhance our understanding of the connection between structural and thermochromic properties of $CuMoO_4$ and related compounds. The ability to tune the thermochromic properties of the material to more desired temperature ranges by the addition of tungsten or zinc ions makes it more promising for applications, for instance, as a cost-effective indicator for monitoring storage/processing conditions of temperature-sensitive products (drugs, vaccines, chemicals, biological materials etc.).

Keywords: $CuMoO_4$, X-ray absorption spectroscopy, EXAFS, XANES, Reverse Monte-Carlo simulations

Contents

Contents **4**

List of abbreviations **5**

1 Introduction **6**

2 X-ray absorption spectroscopy (XAS) **9**
2.1 Basics of XAS 9
2.2 XAS data analysis 10

3 Resonant X-ray emission spectroscopy (RXES) **11**

4 Structure and thermochromic properties of molybdates **12**
4.1 $CuMoO_4$ crystal structure and chromatic properties 12
4.2 Effect of doping 14
4.2.1 An addition of tungsten ions 14
4.2.2 An addition of zinc ions 14

5 Samples and their characterization **15**

6 Overview of the main results **16**
6.1 XAS study of $CuMoO_4$ 16
6.1.1 $CuMoO_4$ at low temperatures 16
6.1.2 $CuMoO_4$ at high temperatures 20
6.2 XAS study of $CuMo_{1-x}W_xO_4$ 23
6.2.1 Composition-dependent $CuMo_{1-x}W_xO_4$ study 23
6.2.2 Temperature-dependent $CuMo_{0.90}W_{0.10}O_4$ study 24
6.3 RXES study at the W L_3-edge of $CuMo_{1-x}W_xO_4$ 26
6.4 XAS study of $Cu_{1-x}Zn_xMoO_4$ 28

7 Summary and conclusions **29**

8 Main theses **32**

Bibliography **33**

Author's publications **37**

Participation in international conferences and workshops **38**

Participation in international schools **40**

Participation in synchrotron experiments **41**

List of abbreviations

BADF	Bond angle distribution function
EA	Evolutionary algorithm
EXAFS	Extended X-ray absorption fine structure
FT	Fourier transformation
HERFD	High energy resolution fluorescence detected
LCA	Linear combination analysis
MS	Multiple-scattering
MSRD	Mean-square relative displacement
RDF	Radial distribution function
RMC	Reverse Monte Carlo
RXES	Resonant X-ray emission spectroscopy
WT	Wavelet transform
XANES	X-ray absorption near edge structure
XAS	X-ray absorption spectroscopy
XES	X-ray emission spectroscopy
XRD	X-ray diffraction

Introduction

General introduction and motivation

Smart materials have properties that can be altered in a controllable manner by external stimuli. For instance, they can respond to light, changes in temperature, pressure, pH, electric and magnetic fields. They are more and more used in different technological applications. One such advanced multifunctional material is copper molybdate ($CuMoO_4$) which has several chromic properties such as thermochromism, piezochromism, tribochromism, halochromism [1–5], being perspective for practicle aplications. Physical properties of $CuMoO_4$ depend on temperature and/or pressure and can also be affected by modifying its chemical composition [1, 2, 6, 7]. Therefore, the structure-property relationship must be understood to learn how to control the functionality of the material. In this thesis, $CuMoO_4$-based thermochromic compounds are investigated to elucidate the structural origin of their optical properties.

Thermochromic materials change their color in response to temperature changes. In the solid inorganic materials, a gradual colour change may occur due to lattice expansion/contraction, which affects the band gap, or a distinct colour change may occur when the structure is modified upon a phase transition [8, p.42].

Pure $CuMoO_4$ has thermochromic properties both at low (100–300 K) and high (400–700 K) temperatures. Above room temperature, the material exists in the α-phase, however at low temperatures, $CuMoO_4$ exhibits a reversible structural phase transition between α and γ phases with a hysteretic behaviour, which is accompanied by a drastic colour change between greenish and brownish [1]. Note that the thermochromic phase transition is strongly affected by chemical composition. For instance, the substitution of Mo^{6+} ions in $CuMoO_4$ by W^{6+} results in the formation of $CuMo_{1-x}W_xO_4$ solid solutions with different temperature response. Similarly, the substitution of Cu^{2+} ions by other divalent ions as Zn^{2+} is possible.

At low temperatures, the considerable optical contrast between the two polymorphic phases makes $CuMoO_4$ appealing for thermochromic applications, for instance, in the fields where one needs to monitor storage/transportation conditions of temperature-sensitive products (food, drugs, vaccines, chemicals, biological materials, etc.). At the same time, such inorganic materials with a thermochromism at high temperatures (above 400 K) attract much attention because of their potential applications for temperature sensing in the ranges where the majority of organic compounds and liquid crystals are unstable [9].

Thermochromic properties of $CuMoO_4$ and related materials are closely connected with the local atomic structure of constituting metal ions, which can

be probed by synchrotron radiation X-ray absorption spectroscopy (XAS). Today synchrotron radiation sources are available worldwide, and X-ray absorption spectroscopy has become an extremely valuable technique for characterising materials. The structural information in XAS is encoded in tiny fluctuations of the X-ray absorption coefficient. It is common to divide the X-ray absorption spectrum into two parts: X-ray absorption near edge structure (XANES), located near the absorption edge, and extended X-ray absorption fine structure (EXAFS), which extends far beyond the edge.

Significant efforts have been made to develop advanced data analysis approaches based on atomistic simulations to improve the reliability, accuracy and amount of structural information that can be extracted from experimental EXAFS spectra. EXAFS probes the structure of a material as averaged over a huge number of "frozen" atomic configurations, in each of which all atoms are slightly displaced from their equilibrium position due to thermal vibrations. Advanced theoretical technique such as reverse Monte Carlo (RMC) provides a natural way to incorporate static and thermal disorder into the structural model and allows one to extract information encoded in X-ray absorption spectra, thus opening new possibilities for the investigation of the structure-property relationships. A complementary technique to XAS is resonant X-ray emission spectroscopy (RXES). It probes a second-order process that includes both X-ray absorption and subsequent emission. From RXES data one can obtain high energy resolution fluorescence detected XAS spectrum (HERFD-XAS spectrum) with a drastically enhanced sensitivity to the local coordination of the absorbing atoms. Thus, a combination of XAS, RXES and theoretical studies might shed light on the correlation between structural and functional properties of such materials as $CuMoO_4$ and its solid solutions.

Aim and objectives of the work

The **aim** of this study is to explore and explain the relationship between the structure and thermochromic properties of copper molybdate ($CuMoO_4$) and its solid solutions with tungsten ($CuMo_{1-x}W_xO_4$) and zinc ($Cu_{1-x}Zn_xMoO_4$) using X-ray absorption and resonant X-ray emission spectroscopies.

The **objectives** of the study are:

- to synthesise and characterize a set of pure $CuMoO_4$, $CuWO_4$, $ZnMoO_4$ compounds and two series of $CuMo_{1-x}W_xO_4$ and $Cu_{1-x}Zn_xMoO_4$ solid solutions;
- to perform temperature and composition-dependent X-ray absorption and resonant X-ray emission spectroscopy studies of $CuMo_{1-x}W_xO_4$ and $Cu_{1-x}Zn_xMoO_4$ solid solutions at synchrotron radiation facilities;
- to analyse experimental X-ray absorption and RXES spectra using modern theoretical approaches based on *ab initio* (full-) multiple-scattering theory and reverse Monte Carlo simulations to obtain structural information on the local environment of absorbing atoms;

- to understand the structure-thermochromic properties relationship in the studied materials.

Scientific novelty of the work

The results of research presented in this thesis are of scientific novelty and have been published in several international journals.

The impact of the W^{6+} ions on the local environment in thermochromic solid solutions $CuMo_{1-x}W_xO_4$ has been studied for the first time by XAS and RXES. It was found that an increase of tungsten content promotes the coordination change of molybdenum atoms from tetrahedral to octahedral that is accompanied by the material colour change from greenish to brownish.

XAS data analysis was performed using modern theoretical approaches, including the RMC method. It was shown that the structural model obtained by the RMC method can be employed to incorporate thermal disorder effects in XANES simulations and to interpret temperature-dependent XANES data. In $CuMoO_4$, a specific dynamic effect has been discovered at the Cu K-edge. It is associated to different rigidity of metal-oxygen coordination polyhedra and influences the thermochromic properties of $CuMoO_4$ above room temperature.

For the first time $Cu_{1-x}Zn_xMoO_4$ were studied by XAS and it was found that, among sampled solid solutions, only $Cu_{0.90}Zn_{0.10}MoO_4$ exhibits the thermochromic phase transition with a hysteretic behaviour. It is explained by the instability of molybdenum coordination which changes from tetrahedral to octahedral under lattice contraction at low temperatures.

Author's contribution

The presented research consists of both experimental and theoretical parts. Main experiments were conducted at international synchrotron radiation facilities. During the period 2015-2021, the author has taken part in 17 experiments using synchrotron radiation that have been carried out at PETRA III (Hamburg, Germany), ELETTRA (Trieste, Italy) and SOLEIL (Paris, France) synchrotrons. In particular, three XAS and one RXES experiments are directly relevant to the present work. Sample synthesis, X-ray diffraction (XRD) measurements and experimental XAS and RXES data processing using different programs was performed by the Author at the Institute of Solid State Physics, University of Latvia (ISSP, UL). All RMC simulations with EvAX code [10] as well as theoretical XANES calculations with FDMNES code [11, 12] have been carried out by the Author at the Latvian SuperCluster facility [13]. Interpretation of the obtained results was performed in collaboration with the supervisor.

The Author has participated in 9 international summer schools during 2014-2021. The results of the research have been presented at 20 international conferences and workshops. The main results have been published in 21 SCI papers, and the Author is the first contributor for 11 of them. 8 scientific publications are directly related to this thesis. The h-index of the Author is 7.

X-ray absorption spectroscopy (XAS)

2.1. Basics of XAS

The absorption phenomenon of electromagnetic radiation is described by the Beer-Lambert law: $I(E) = I_0(E)e^{-\mu(E)x}$, where $I_0(E)$ is the incident radiation intensity, x is the sample thickness, $I(E)$ is the intensity of radiation transmitted through the sample, and $\mu(E)$ is the linear absorption coefficient describing the fraction of an X-ray beam that is absorbed per unit thickness of the absorber. A typical experimental setup for XAS measurements at the synchrotron is shown in Fig. 2.1.1.

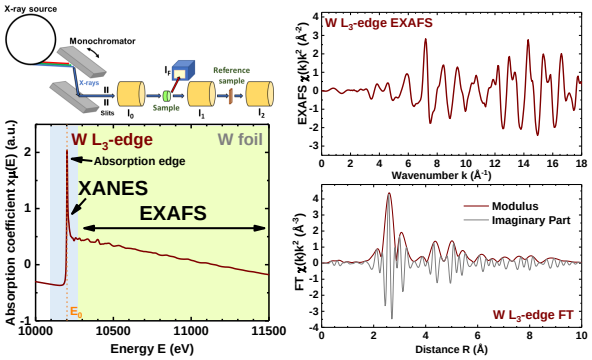

Figure 2.1.1: ***A scheme of experimental setup for XAS measurements; X-ray absorption spectrum*** $x\mu(E)$ ***of tungsten foil at the W*** L_3 ***absorption edge; extracted EXAFS*** $\chi(k)k^2$ ***spectrum and corresponding Fourier transform.***

The flux of photons propagating through the material is reduced exponentially due to the interactions of the incident radiation with atoms. However, the smooth energy dependence of the absorption coefficient, is interrupted at specific energies by a sharp rise in the absorption - absorption edges. They occur when the incident X-ray energy is equal to that of the binding energy of an electron, which is excited [14]. Depending on the electronic level being involved ($1s$, $2s$, $2p_{1/2}$, $2p_{3/2}$, etc.), the absorption edges are denoted as K, L_1, L_2, L_3, etc. edges. Thus, one can select the element to probe by tuning the X-ray energy to the desired absorption edge region. An example of the W L_3-edge X-ray absorption spectrum of a tungsten foil is shown in Fig. 2.1.1.

The experimental EXAFS spectrum $\chi(k)$ contains information on the local atomic structure around the absorbing atom, including pair and many-atom correlation functions. Pair correlation functions, also known as radial

distribution functions (RDFs) $g(R)$, contribute into EXAFS through the single-scattering processes. Many-atom correlation functions give origin to the multiple-scattering (MS) events when the photoelectron scatters from more than one atom. Therefore, the real-space MS theory [15] is used for a quantitative description of EXAFS. The different oscillation frequencies present in $\chi(k)$ correspond to contributions from atoms located at different distances (coordination shells) or from higher-order scattering paths. The direct Fourier transform (FT) allows one to transfer EXAFS spectrum into the R-space and, thus, to visualize contributions from different scattering paths (Fig. 2.1.1).

2.2. XAS data analysis

Though the XANES and EXAFS parts of X-ray absorption spectra have the same physical origin, their distinction is convenient for the interpretation. XANES contains information on the chemical state and symmetry around the absorbing atom. Most often XANES region is used as a fingerprint to identify chemical species in complex materials. However, significant efforts have been made to develop theory for interpretation of XANES [12].

EXAFS analysis gives more detailed information on the local atomic environment. A conventional EXAFS analysis [15] based on nonlinear least-square fitting most often can be used only for the first coordination shell analysis without further significant approximations due to MS contributions at longer distances. Data analysis is challenging also if large disorder (static or thermal) is present in the material and the bond-lengths cannot be approximated with a Gaussian distribution. One can try to solve this problem by the mathematical model employing the RDFs $g(R)$ with a more complex shape or by the expansion of $g(R)$ in the cumulant series [16]. An alternative is the regularization approach [17] or simulation-based EXAFS analysis, for instance, using molecular dynamics [18, 19], Monte Carlo [20] and reverse Monte Carlo (RMC) [21] methods. The RMC method with an evolutionary algorithm (EA) approach implemented in the EvAX code and used in this thesis was developed by J. Timoshenko at the EXAFS spectroscopy laboratory (ISSP, UL) [10, 22].

The RMC/EA method is based on the iterative random changes (Metropolis algorithm [20]) in the structural model, aimed to minimize the difference between the Morlet wavelet transforms (WTs) [23] of the experimental and calculated configuration-averaged EXAFS spectra. The comparison in k- and R-spaces simultaneously using WTs gives better control over the agreement between experimental and calculated spectra. EA makes these calculations computationally more efficient. Thus, it is possible to include in the analysis a larger number of photoelectron scattering paths and distant coordination shells considering all significant MS contributions. Furthermore, EvAX code allows one to construct a structural model, consistent with the experimental EXAFS data, obtained at several absorption edges.

Resonant X-ray emission spectroscopy (RXES)

X-ray emission spectroscopy (XES) is a second-order optical process that includes X-ray absorption and subsequent emission. It is common to divide the XES into two categories. The first one is normal XES or non-resonant XES, when the core electron is excited to the high-energy continuum. The second category is a resonant XES (RXES) when the incident X-ray energy "resonates" with the excitation threshold of the core electron [24, p.335].

Since the efficiency of the X-ray emission is low, the signal-to-background ratio plays a significant role. The experimental setup requires high-intensity and tunable X-ray photon source such as a synchrotron and an X-ray spectrometer based on perfect-crystal Bragg optics [25]. Such spectrometers have an energy bandwidth similar to the lifetime induced broadening of the corresponding core level and allows one to obtain superior resolution compared to conventional XANES. An example of the experimental setup for hard RXES is shown in Fig. 3.0.1(a). During the experiment, the intensity of both incident and emission X-rays is recorded and after the signal processing a so-called RXES plane is obtained (Fig. 3.0.1(b)) [26].

By selectively extracting the emitted photon intensity in the narrow energy range close to the emission line (that corresponds to the transitions between energy levels with long lifetimes), one can obtain high energy resolution fluorescence detected XAS spectrum (HERFD-XAS spectrum) with a drastically enhanced sensitivity to the local coordination of the neighbouring atoms. The X-ray emission spectra obtained by scanning the emitted radiation slightly below [27] or above the absorption edge are called off-resonant X-ray emission spectra [28].

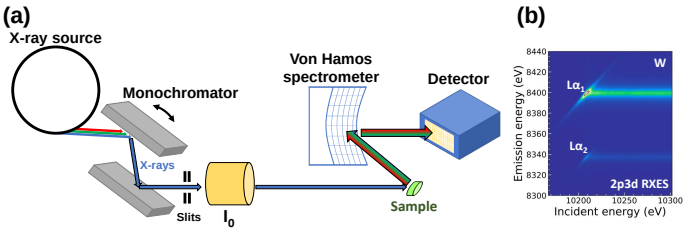

Figure 3.0.1: ***A schematic representation of the experimental setup for RXES measurements (a) and tungsten 2p3d RXES plane (b).*** *Two focusing mirrors located after the monochromator are not shown for clarity.*

Structure and thermochromic properties of molybdates

4.1. $CuMoO_4$ crystal structure and chromatic properties

Structure, optical, electrical, and magnetic properties of $CuMoO_4$ were studied previously in detail in [1, 6, 9, 29–31]. The pressure–temperature phase diagram (Fig. 4.1.1) for $CuMoO_4$ was determined based on a single crystal XRD data by Wiesmann *et al.* in [1]. The first order α-to-γ phase transition occurs upon cooling the material below $\sim$200 K (or by applying pressure above $\sim$0.2 GPa). In addition to the colour change from green to brown, the α-to-γ phase transition is accompanied by an unit cell volume decrease of 12–13% [1]. The phase transition was also studied previously using optical spectroscopy, differential scanning calorimetry, magnetic susceptibility, and dielectric measurements [6, 9, 32]. It was found that the transition has hysteretic a behaviour so that higher temperature is required to promote the γ-to-α transition than α-to-γ. Both phases are separated by a region where they coexist.

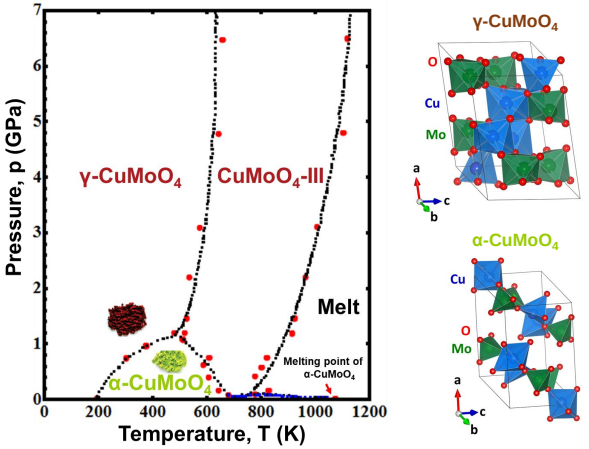

Figure 4.1.1: ***Pressure-temperature phase diagram for*** **$CuMoO_4$** ***(adapted from [1]) and the unit cells of*** **γ-$CuMoO_4$** ***and*** **α-$CuMoO_4$**.

At ambient pressure, $CuMoO_4$ remains in the triclinic $P\bar{1}$ symmetry up to the melting point temperature ($\sim$1070 K) [1]. There are significant differences in the crystallographic structure of α and γ phases (Fig. 4.1.1). The γ-phase of $CuMoO_4$ is built up of distorted CuO_6 and MoO_6 octahedra [1, 30], while α-$CuMoO_4$ is composed of distorted CuO_6 octahedra, CuO_5 square-pyramids, and

distorted MoO_4 tetrahedra [1, 33]. The first-order ($Cu^{2+}[3d^9]$) and second-order ($Mo^{6+}[4d^0]$) Jahn-Teller effects are responsible for the distortion of CuO_6 and MoO_6 octahedra. The unit cell of $CuMoO_4$ structure in both phases contains six formula units (Z=6) with three non-equivalent copper (Cu1, Cu2, Cu3) and molybdenum (Mo1, Mo2, Mo3) atoms, which have different local environments [1, 30]. Thus, the unit cell of $CuMoO_4$ consist of 36 atoms, and the structural analysis is challenging.

It is worth mentioning that a colour change from green to brown but of different origin occurs in pure α-phase of $CuMoO_4$ upon heating up to ~673 K [9].

The green colour of $CuMoO_4$ is caused by the optical transmission window in the energy range of ~1.9–2.5 eV (500–650 nm) (Fig. 4.1.2(a)) [9]. The chromatic properties of $CuMoO_4$ are associated with the interplay between two optical absorption bands. The first band, located in the red spectral range above ~650 nm, is related to the copper $3d^9 \rightarrow 4p$ [9] or d-d transitions [6, 29, 34]. The second band, located in the blue spectral range below ~500 nm, is still not fully understood. It is attributed to the oxygen-to-metal ($O^{2-} \rightarrow Mo^{6+}$ or $O^{2-} \rightarrow Cu^{2+}$) [6, 9, 29, 34] or $Cu^{2+} \rightarrow Mo^{6+}$ [35] charge transfer processes. Nevertheless, when the temperature increases from 296 K to 673 K, the transmission window shrinks due to the blue band shift towards longer wavelengths (Fig. 4.1.2(a)), and the crystal changes both transmittance and colour [9].

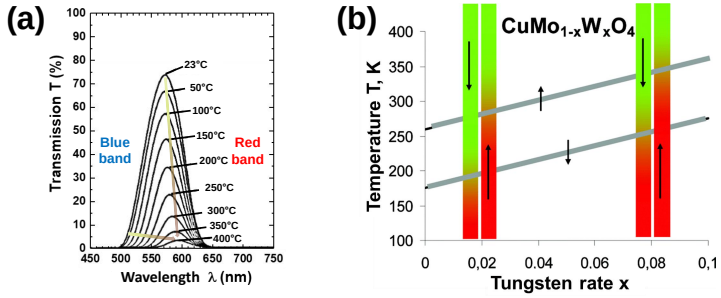

Figure 4.1.2: ***Temperature-dependent optical transmission spectra of*** **$CuMoO_4$** ***(adapted from [9])(a); Correlation between the phase transition temperatures (gray lines) and tungsten rate x in $CuMo_{1-x}W_xO_4$ solid solutions (adapted from [6]) (b).***

4.2. Effect of doping

4.2.1. An addition of tungsten ions

Several studies have revealed that the thermochromic properties can be strongly affected by tungsten addition to $CuMoO_4$, resulting in a formation of $CuMo_{1-x}W_xO_4$ solid solutions [2, 3, 6, 7, 36]. Depending on the tungsten concentration, phases isostructural to high pressure phases of $CuMoO_4$ (α-$CuMoO_4$, γ-$CuMoO_4$ and $CuMoO_4$-III) with different Cu, Mo and W coordination can be obtained [1, 36, 37]. Furthermore, the $\alpha \leftrightarrow \gamma$ phase transition temperature depends strongly on tungsten concentration and becomes higher when the tungsten content increases (Fig. 4.1.2(b)) [2, 6, 7, 37]. Tungsten concentration above $\sim$15% in $CuMo_{1-x}W_xO_4$ solid solutions leads to wolframite-type ($CuMoO_4$-III) phase with the octahedral coordination of metal ions and do not exhibit pronounced thermochromic behaviour but may be interesting for other applications.

4.2.2. An addition of zinc ions

There are only a few papers reporting the effect of substituting Cu^{2+} ions in $CuMoO_4$. The closest ionic radius to Cu^{2+} (0.73 Å) is for Zn^{2+} (0.74 Å) ion. Indeed, copper and zinc molybdates form a complete solid solution series $Cu_{1-x}Zn_xMoO_4$ ($0 \leq x \leq 1$) [38, 39]. Note that α-$ZnMoO_4$ phase is isostructural to α-$CuMoO_4$ [40] and is stable in the whole temperature range till its decomposition temperature of 1280 K [39]. α-$ZnMoO_4$ is composed of distorted ZnO_6 octahedra, ZnO_5 square-pyramids and MoO_4 tetrahedra [38].

Magnetic susceptibility measurements of $Cu_{1-x}Zn_xMoO_4$ ($0 \leq x \leq 0.1$) samples reported in [41] indicate on the shift of the phase transition point to the lower temperatures with increasing Zn content. Yanase *et al.* [42] studied the thermochromic phase transition in the $CuMo_{0.94}W_{0.06}O_4$ material doped with small amount of Zn ($0 \leq x \leq 0.05$). The results showed that the substitution of Cu^{2+} by Zn^{2+} reduces the phase transition temperature of $CuMo_{0.94}W_{0.06}O_4$ and stabilizes the α-phase. Thus, the phase change occurs in the temperature range of 303–343 K. Recently, structural, morphological and optical properties of solid solutions with large Zn content ($0.92 \leq x \leq 1.00$) were studied [43]. In [44], luminescence and pigment properties of $Cu_{0.10}Zn_{0.90}MoO_4$ were also reported.

A deep understanding of the structure-thermochromic property relationship in molybdates requires detailed information on the temperature dependence of their local atomic structure, which can be obtained using X-ray absorption spectroscopy. This question is one of the goals of the thesis and is addressed in the further sections.

Samples and their characterization

Polycrystalline powders of $CuMo_{1-x}W_xO_4$ solid solutions (x = 0, 0.04, 0.06, 0.10, 0.12, 0.15, 0.20, 0.50, 0.75, 1.00) were synthesized using a simple solid-state route by heating an appropriate mixture of CuO and MoO_3 powders with added stoichiometric amount of WO_3 at 650°C in the air for 8h followed by cooling down naturally to the room temperature. One group of as-prepared samples with $x \leq 0.15$ had greenish colour, and the second group with $x \geq 0.20$ was brownish (Fig. 5.0.1(a)). The phase of as-prepared powders was confirmed by X-ray powder diffraction and micro-Raman spectroscopy.

An example of the γ-$CuMo_{0.96}W_{0.04}O_4$ sample stabilized at room temperature by treatment α-$CuMo_{0.96}W_{0.04}O_4$ powder sample at 77 K in liquid nitrogen (cryogenic quenching) is shown in Fig. 5.0.1(b).

Polycrystalline $Cu_{1-x}Zn_xMoO_4$ powders (x = 0.10, 0.25, 0.50, 0.75, 0.90, 1.00) were synthesized similarly using a solid-state reaction method. Photos of selected samples are shown in Fig. 5.0.1(c).

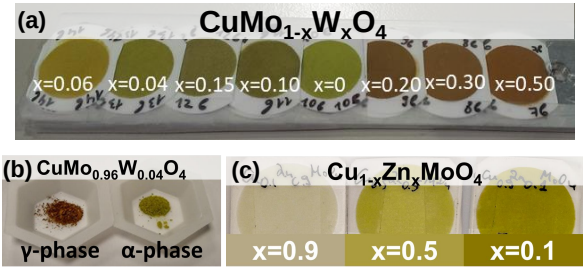

Figure 5.0.1: ***Photos of selected samples (see text for details).***

X-ray absorption experiments were performed within four beamtime projects at PETRA III (Germany) and ELETTRA (Italy) synchrotron radiation sources. Low-temperature (from 10 K to 300 K) XAS experiments for $CuMo_{1-x}W_xO_4$ and $Cu_{1-x}Zn_xMoO_4$ samples were conducted at the HASYLAB PETRA III P65 undulator beamline [45]. High-temperature measurements were performed at the ELETTRA XAFS bending-magnet beamline [46] in the temperature range from 296 K to 973 K. The fourth synchrotron radiation experiment (RXES measurements) was performed at the HASYLAB PETRA III P64 undulator beamline [47]. Experimental details can be found in [28, 48–50].

Overview of the main results

6.1. XAS study of $CuMoO_4$

6.1.1. $CuMoO_4$ at low temperatures [1]

In this section, the *in situ* temperature-dependent (10–300 K) Cu and Mo K-edge XAS study of a thermochromic phase transition between brownish γ-$CuMoO_4$ and greenish α-$CuMoO_4$ is briefly reported. The Cu and Mo K-edge XANES and EXAFS parts of the X-ray absorption spectra were isolated and analysed separately.

XANES analysis

The experimental Mo K-edge XANES spectra corresponding to γ-$CuMoO_4$ at 10 K and α-$CuMoO_4$ at 300 K are shown in Fig. 6.1.1(a). The pre-edge peak at the Mo K-edge is visible at ~20000 eV. It corresponds to the 1s(Mo)→4d(Mo)+2p(O) transition. The amplitude of the pre-edge peak depends on the distortion degree of the MoO_6 octahedra and 4d(Mo)/2p(O) orbital mixing. It is the largest for tetrahedral MoO_4 coordination (Fig. 6.1.1(b)). Therefore, it can be used to trace the α-to-γ phase transition in $CuMoO_4$.

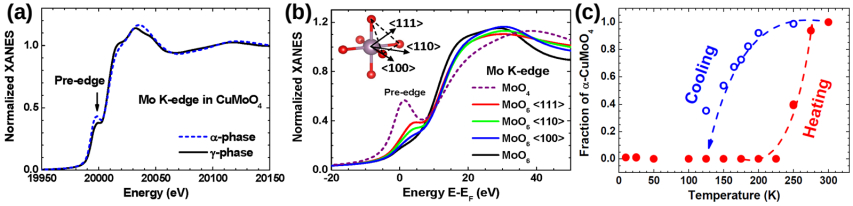

Figure 6.1.1: ***The Mo K-edge XANES of α-$CuMoO_4$ and γ-$CuMoO_4$ phases:*** *Experimental Mo K-edge XANES of α-$CuMoO_4$ (at 300 K) and γ-$CuMoO_4$ (at 10 K) phases (a). Calculated Mo K-edge XANES for regular MoO_4 tetrahedron and distorted and regular MoO_6 octahedra. Numbers in brackets indicate the direction of molybdenum ion displacement from the center illustrated in the inset (b). Temperature dependence of the fraction of α-$CuMoO_4$ phase (c).*

[1] The material, presented in this section, has been published as: I. Jonane, A. Cintins, A. Kalinko, R. Chernikov, A. Kuzmin, **X-ray absorption near edge spectroscopy of thermochromic phase transition in $CuMoO_4$**, Low Temp. Phys. 44 (**2018**) 568-572 and I. Jonane, A. Cintins, A. Kalinko, R. Chernikov, A. Kuzmin, **Probing the thermochromic phase transition in $CuMoO_4$ by EXAFS spectroscopy**, Phys. Status Solidi B 255 (**2018**) 1800074:1-5.

A fraction of α-$CuMoO_4$ phase at each temperature shown in Fig. 6.1.1(c) was evaluated using a linear combination of the lowest temperature (10 K) and the highest temperature (300 K) Mo K-edge XANES spectra. The results show that the γ-to-α phase transition takes place in $CuMoO_4$ upon heating in the temperature range between ~230 and 280 K, whereas the α-to-γ phase transition occurs at a lower temperature between ~120 and 200 K. The hysteresis loop of the phase transition is well observed. The two temperatures $T_{1/2H}$ and $T_{1/2C}$ corresponding to about 50% of the α and γ phases in the sample upon heating and cooling, respectively, are equal to $T_{1/2H} \approx 255$ K and $T_{1/2C} \approx 143$ K. The width of the hysteresis loop is defined as $\Delta T_{1/2} = T_{1/2H} - T_{1/2C} = 112$ K.

EXAFS experimental data

Experimental Cu and Mo K-edge EXAFS $\chi(k)k^2$ spectra of $CuMoO_4$ were extracted following the conventional procedure [51] using the Athena [52] package. The EXAFS spectra and their FTs calculated in the k-space range of 2.5-14.5 $Å^{-1}$ at selected temperatures are shown in Fig. 6.1.2.

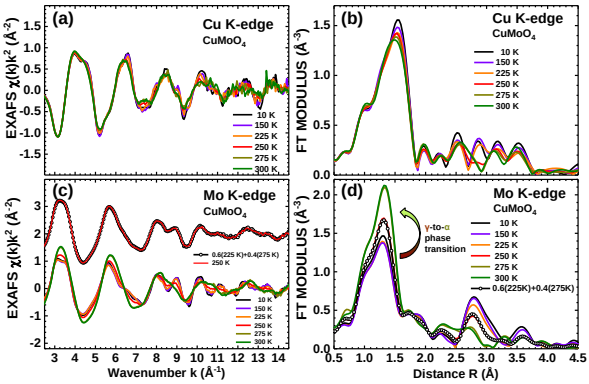

Figure 6.1.2: ***Temperature-dependent experimental EXAFS data for crystalline*** **$CuMoO_4$** ***at the Cu (a) and Mo (c) K-edge and their Fourier transforms (b,d)*** *(only modulus is shown). A weighted sum of the two Mo K-edge EXAFS spectra recorded at 225 and 275 K is shown by open circles and it is compared with the experimental EXAFS spectrum measured at 250 K in panels (c,d).*

One can see that the Cu K-edge spectra are weakly affected during temperature increase, however, at 250 K some changes occur, that can be attributed to the transition from CuO_6 octahedra to CuO_5 square-pyramids. At the same time, the Mo K-edge is drastically affected during the phase transition because of the changes in molybdenum coordination from octahedral to tetrahedral. The changes in the atomic structure of the material occur in all coordination shells around Mo, leading to a variation of peaks in FTs.

Recovery of structural information encoded in EXAFS data for such low-symmetry materials as $CuMoO_4$ is challenging. Here we present two approaches to extract this information based on a regularization-like technique and the RMC/EA method.

EXAFS analysis using regularization-based technique

The analysis of the Fourier-filtered first coordination shell Mo K-edge EXAFS using a regularization-like method implemented in the EDARDF code [17] resulted in a good agreement with the experimental data and allowed to obtain temperature-dependent RDFs $g_{\mathrm{Mo-O}}(R)$ of molybdenum atoms (Fig. 6.1.3(a,b)).

The group of the nearest four oxygen atoms is sensitive to structural distortions as reflected by the peak broadening and was used to extract MSRD (mean-square relative displacement) σ^2 values (Fig. 6.1.3(c)). Significant decrease in the MSRD factor values from $\sim$0.010 to $\sim$0.005 Å^2 is observed above $\sim$225 K, indicating on the phase transition and changes in the local environment of Mo atoms, i.e., transformation from strongly distorted octahedral environment in γ-$CuMoO_4$ to less distorted tetrahedral in α-$CuMoO_4$. Furthermore, the variation of the MSRD in the γ-phase below 225 K is negligible being within the error bars due to the dominant role of static distortions.

The temperature dependence of the RDFs $g_{\mathrm{Mo-O}}(R)$ and obtained MSRD factor σ^2 values suggest that the γ-to-α phase transition occurs gradually within a temperature range of 225–275 K, in agreement with the results of previous studies [2, 6, 32] and the linear combination analysis (LCA) of the Mo K-edge XANES.

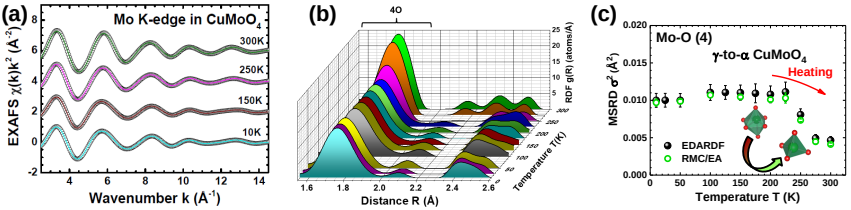

Figure 6.1.3: ***Results of EXAFS data analysis with regularization-like method:*** *Comparison of the experimental (open circles) and calculated by the regularization-like method [17] (solid lines) Mo K-edge EXAFS $\chi(k)k^2$ spectra for the first coordination shell of molybdenum atoms in $CuMoO_4$ at selected temperatures (a). Obtained temperature-dependent RDFs $g_{\mathrm{Mo-O}}(R)$ in $CuMoO_4$. The first peak due to the four nearest oxygen atoms is indicated (b). Temperature dependence of the MSRD factor σ^2 for the four shortest Mo–O interatomic distances in $CuMoO_4$ obtained from regularization-like (EDARDF code [17]) and RMC/EA methods (c).*

EXAFS analysis based on the RMC/EA approach

Further EXAFS data analysis by the RMC/EA method allowed us to reconstruct temperature-dependent three-dimensional structure models of $CuMoO_4$, consistent with the experimental data simultaneously at the Cu and Mo K-edges.

The obtained RMC/EA fits for $CuMoO_4$ at selected temperatures are shown in Fig. 6.1.4(a-d). One can see that the experimental EXAFS spectra of $CuMoO_4$ at 200 K and 300 K are well described by the structural models of γ and α phases, respectively. At the same time, the structural models of both α and γ phases give reasonable agreement with the experimental data at T=250 K, indicating the coexistence of the two phases in close ratio. This conclusion agrees with the LCA results (Fig. 6.1.1(c)) suggesting the presence of the 60% and 40% of γ- and α-$CuMoO_4$ phases, respectively [53].

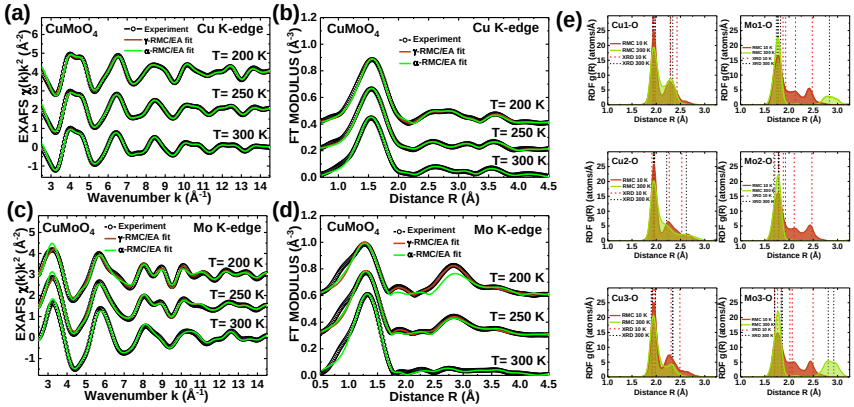

Figure 6.1.4: ***Results of RMC/EA calculations for the Cu and Mo K-edges in* $CuMoO_4$ *at selected temperatures****: the experimental and calculated EXAFS spectra $\chi(k)k^2$ using α- and γ-$CuMoO_4$ initial structure models (a,c) and the corresponding Fourier transforms (b,d). Radial distribution functions for three non-equivalent Cu–O, Mo–O atom pairs in $CuMoO_4$ calculated from the atom coordinates of the RMC/EA models (e). Dashed vertical lines show interatomic distances according to diffraction data [1].*

Temperature-dependent partial RDFs around copper and molybdenum atoms were calculated from the atom coordinates of the RMC/EA models. Distributions corresponding to the first coordination shell at 10 K and 300 K are compared in Fig. 6.1.4(e). Note that one can distinguish three non-equivalent crystallographic sites of Cu and Mo atoms with different local environments. The MSRD values for Mo–O atom pairs obtained in RMC/EA calculations coincide with those obtained from the regularization method (Fig. 6.1.3(c)).

6.1.2. $CuMoO_4$ at high temperatures[2]

In this section, the relationship between the structure and thermochromic properties of $CuMoO_4$ observed at high temperatures is summarized. Note that no structural phase transition occurs in $CuMoO_4$ at high temperatures (> 300 K), and it always remains in the α-phase. XAS at the Cu and Mo K-edges was used to investigate the effect of heating on the local atomic structure and lattice dynamics in α-$CuMoO_4$ in the temperature range from 296 to 973 K.

XAS experimental data

Experimental data (Fig. 6.1.5) indicate that the local environment of copper atoms is more affected during heating than that of molybdenum atoms. Furthermore, the thermal disorder affects strongly not only the Cu K-edge EXAFS, but also XANES region.

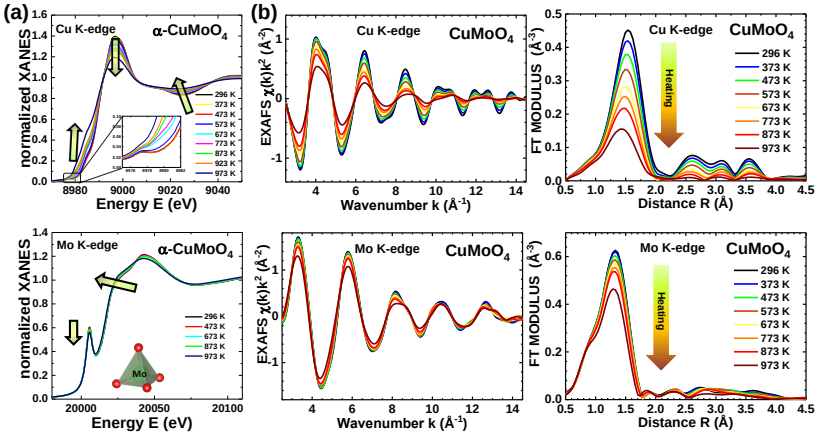

Figure 6.1.5: ***Temperature-dependent experimental Cu and Mo K-edge XANES (a) and EXAFS spectra with their Fourier transforms for α-$CuMoO_4$ (b).***

The pre-edge peak at the Cu K-edge located at $\sim$ 8978 eV is very weak. Its origin is due to the 1s(Cu)$\rightarrow$3d(Cu)+2p(O) transition [54], which is weaker in six-fold or five-fold coordination than in the tetrahedral one. Note that the small intensity of the pre-edge peak is mainly due to the limited number of unoccupied ($Cu^{2+}(3d^9)$) states. The Cu K-edge pre-edge peak becomes even less pronounced at higher temperatures (Fig. 6.1.5). Upon the temperature increase, the Cu K-edge XANES spectra show a rather strong response – the shoulder appears at $\sim$ 8985 eV, the main peak at $\sim$ 8997 eV becomes smaller, and some increase

[2]The material, presented in this section, has been published as: I. Jonane, A. Anspoks, G. Aquilanti, A. Kuzmin, **High-temperature X-ray absorption spectroscopy study of thermochromic copper molybdate**, Acta Mater. 179 (**2019**) 26-35.

of the absorption occurs at $\sim$ 9025 eV. Such strong changes in the Cu K-edge XANES cannot be related simply to the lattice expansion.

Theoretical XANES calculations performed for the equilibrium static structures at different temperatures [1] taking into account the thermal expansion of the lattice give close XANES spectra (Fig. 6.1.7(e)). The only difference is in the oscillation frequency above the absorption edge due to the expected increase of interatomic distances. Thus, equilibrium static structure models are not able to reproduce temperature induced variation in the XANES data observed in the experiment and thermal disorder should be explicitly included in the structural model.

Atoms in the structural models obtained from EXAFS spectra using the RMC calculations are displaced from their equilibrium positions to reproduce thermal disorder and include correlation effects in atomic motion. Therefore, these atomic coordinates were used to interpret XANES temperature dependence.

Results of RMC/EA calculations

The RMC/EA simulations allowed us to perform accurate and simultaneous analysis of the Cu and Mo K-edge EXAFS spectra of polycrystalline α-$CuMoO_4$. The obtained 3D structure models include thermal disorder effects. At the same time, they are able to reproduce the Wyckoff positions of atoms in agreement with known diffraction data [1] (Fig. 6.1.6).

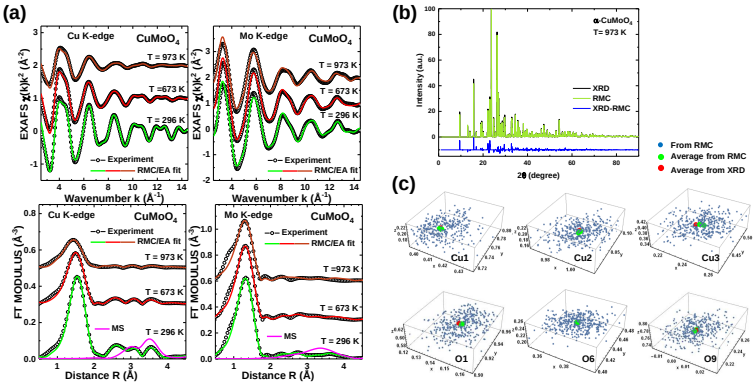

Figure 6.1.6: ***The results of RMC/EA-EXAFS calculations for α-$CuMoO_4$ at selected temperatures****: the Cu and Mo K-edges EXAFS spectra $\chi(k)k^2$ and their Fourier transforms (a). Comparison of diffraction pattern corresponding to structural model for α-$CuMoO_4$ at 973 K obtained in RMC/EA simulations with XRD data (b). An illustrative comparison of the atomic positions (blue) of six non-equivalent atoms in the unit cell obtained in the RMC/EA-EXAFS simulations at 973 K with their Wyckoff positions (red) from the diffraction data [1] and evaluated from the RMC/EA simulations (green).*

The structural models obtained by RMC/EA simulations were used to calculate the configuration-averaged Cu K-edge XANES using the *ab initio* full-multiple-scattering theory (FDMNES code) [11, 12]. The obtained spectra are shown in Fig. 6.1.7 (a). One can see that some configurations produce quite different XANES, but the configuration-averaged XANES are close to the experimental data (Fig. 6.1.7(c,d)). With these structural models it is possible to reproduce the experimentally observed temperature dependence, including the behaviour of the main peak at $\sim$ 8997 eV and the fine structure at $\sim$ 9025 eV.

More detailed analysis allowed us also to interpret the variation in the Cu K-edge shoulder at $\sim$ 8985 eV which is related to the axial oxygen atoms. Namely, while the MoO_4 tetrahedra behave mostly as the rigid units, a reduction of correlation in atomic motion between copper and its axial oxygen atoms occurs upon temperature increase (Fig. 6.1.7(f)). This dynamic effect is the main cause for the temperature-induced changes in the $O^{2-} \rightarrow Cu^{2+}$ charge transfer processes and, thus, is the origin of the thermochromic properties of α-$CuMoO_4$ upon heating [48].

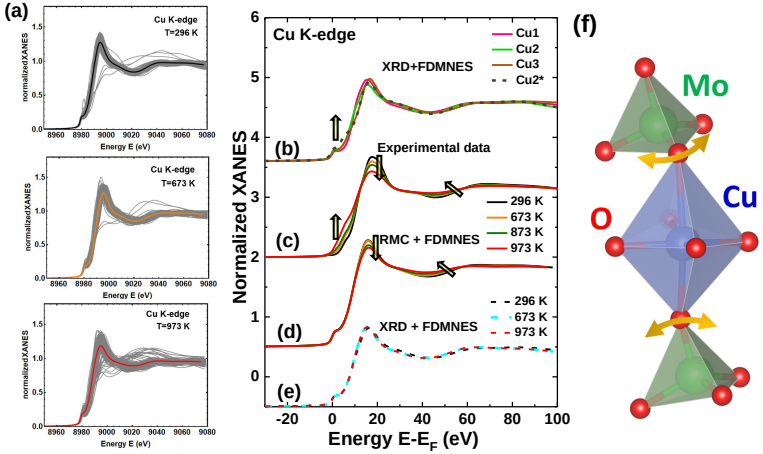

Figure 6.1.7: ***The Cu K-edge XANES spectra of*** **α-$CuMoO_4$***: The calculated Cu K-edge XANES spectra for individual copper atoms in the supercell (gray lines) and the configuration-averaged XANES spectra (coloured lines) (a). The XANES spectra calculated for non-equvalent atoms in the average structure at 296 K known from XRD measurements. The XANES spectrum for Cu2* corresponds to the case of the Cu2 atom without two axial oxygen atoms (b). The experimental XANES at selected temperatures (c). The averaged XANES spectra calculated for the RMC/EA structure models at selected temperatures (d). The averaged XANES spectra calculated for the XRD structure models at selected temperatures taking into account the lattice expansion (e). Illustration of correlation reduction in atomic motion between copper and axial oxygen atoms (f).*

6.2. XAS study of $CuMo_{1-x}W_xO_4$

This section is devoted to the effect of tungsten concentration on the structure and properties of $CuMo_{1-x}W_xO_4$. Special attention is paid to the $CuMo_{0.90}W_{0.10}O_4$ compound, since it seems to be the most attractive solid solution among the series for potential practical applications due to the γ-to-α phase transition in the temperature range between 0 and 100°C [4, 6].

Multi-edge XAS was used to probe a variation of the local atomic structure in $CuMo_{1-x}W_xO_4$ ($0 \leq x \leq 1$) solid solutions at room temperature and in $CuMo_{0.90}W_{0.10}O_4$ in the temperature range of 10–300 K.

6.2.1. Composition-dependent $CuMo_{1-x}W_xO_4$ study

The experimental EXAFS spectra of $CuMo_{1-x}W_xO_4$ (Fig. 6.2.1) show clear dependence on x related to the large difference in atomic masses and electron configurations of Mo and W atoms.

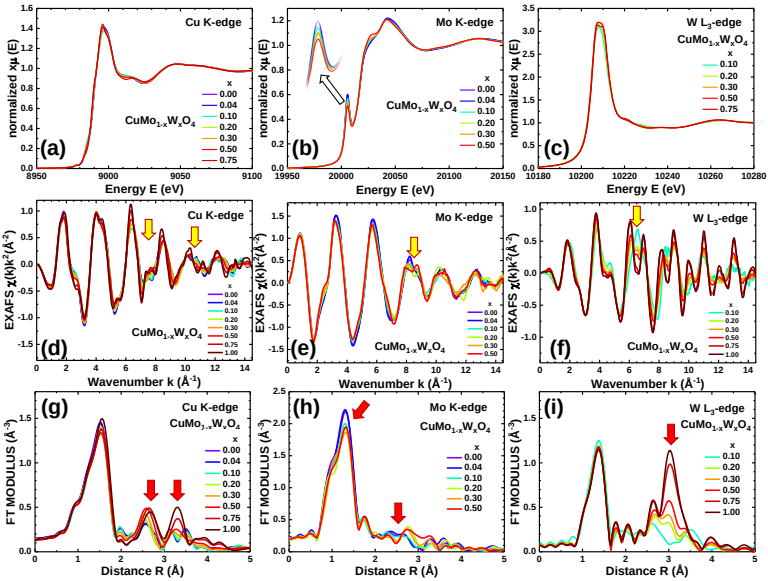

Figure 6.2.1: ***The experimental Cu, Mo K-edge and W L_3-edge normalized XANES (a-c) and EXAFS $\chi(k)k^2$ (d-f) spectra and their Fourier transforms (g-i) for $CuMo_{1-x}W_xO_4$ solid solutions calculated in the k-space range of 2.5-14.5 $Å^{-1}$ with Athena program.***

The structural models for solid solutions with x = 0.20, 0.30, 0.50, 0.75 were obtained from the simultaneous analysis of EXAFS spectra measured at several absorption edges (Cu and Mo K-edges and W L_3-edge) by the RMC/EA method. It was shown that MS effects play an important role in the analysis of

$CuMo_{1-x}W_xO_4$ solid solutions and should be taken into account to describe accurately the contributions from the outer coordination shells. A detailed analysis of the partial RDFs around absorbing metal atoms and the bond angle distribution functions (BADFs) gave information on the degree of distortion of the coordination shells and its dependence on the composition.

Axial distortion of CuO_6 octahedra results in a monomodal BADF of ∠O–Cu–O with an average angle value of $\varphi \approx 88°$. At the same time, off-center displacement of Mo or W atoms from the center of the octahedra leads to bimodal BADFs of ∠O–Mo–O and ∠O–W–O with maxima at $\varphi \approx 80°$ and 96°, respectively. Molybdenum and tungsten atoms are octahedrally coordinated by oxygen atoms in solid solutions with $x \geq 0.20$; however, MoO_6 octahedra are somewhat more distorted than WO_6. For both metals the distorted octahedra consist of three short and three long metal–oxygen bonds, and the group of the nearest three oxygen atoms has narrow distribution. The ability of molybdenum atoms to adopt a locally distorted environment allows them to adjust to the solid solution structure determined by tungsten-related sublattice.

6.2.2. Temperature-dependent $CuMo_{0.90}W_{0.10}O_4$ study [3]

$CuMo_{0.90}W_{0.10}O_4$ solid solution exhibits thermochromic properties similar to pure $CuMoO_4$. However, we observed that the addition of 10 mol% of tungsten to $CuMoO_4$ induces local distortions and stabilizes the γ-phase, leading to an increase of the phase transition temperature by ∼50–100 K (Fig. 6.2.2).

The partial RDFs for Cu–O, Mo–O and W–O atom pairs, calculated from the atomic coordinates of the RMC/EA models of $CuMo_{0.90}W_{0.10}O_4$, are shown in Fig. 6.2.3. At low temperature (50 K) in γ-phase, tungsten atoms have distorted octahedral coordination close to that of molybdenum. At 300 K (in α-phase), when the coordination of Mo atoms becomes tetrahedral, W atoms tend to have a more distorted environment. By comparing Mo–O and W–O RDFs (Fig. 6.2.3), one can see that in the W–O distribution, there is an additional group of oxygen atoms at about 2.1 Å, and the next group of oxygen atoms at 2.8 Å is slightly displaced and split. Furthermore, the RMC/EA calculations at the W L_3-edge for α-$CuMo_{0.90}W_{0.10}O_4$ using the structure model corresponding to γ-phase (tungsten in the distorted octahedral environment) give slightly better agreement with the experimental data, however, the shape of the W–O distribution is quite close to that obtained using α-phase initial structure model.

[3] The results related to $CuMo_{0.90}W_{0.10}O_4$, have been published as I. Jonane, A. Cintins, A. Kalinko, R. Chernikov, A. Kuzmin, **Low temperature X-ray absorption spectroscopy study of $CuMoO_4$ and $CuMo_{0.90}W_{0.10}O_4$ using reverse Monte-Carlo method**, Rad. Phys. Chem. 175 (**2020**) 108411.

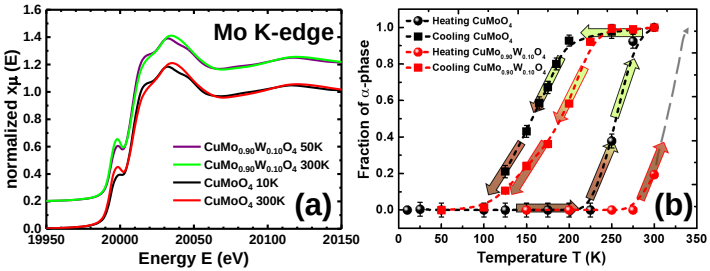

Figure 6.2.2: ***Experimental Mo K-edge XANES of*** $\mathbf{CuMoO_4}$ ***and*** $\mathbf{CuMo_{0.90}W_{0.10}O_4}$ ***at 300 K (α-phase) and 10 K/50 K (γ-phase)*** *(a). Temperature dependence of the fraction of α-phase in* $CuMoO_4$ *and* $CuMo_{0.90}W_{0.10}O_4$ *upon heating and cooling obtained from the LCA analysis of the Mo K-edge XANES spectra (b). The gray dashed arrow is an extrapolation above the room temperature.*

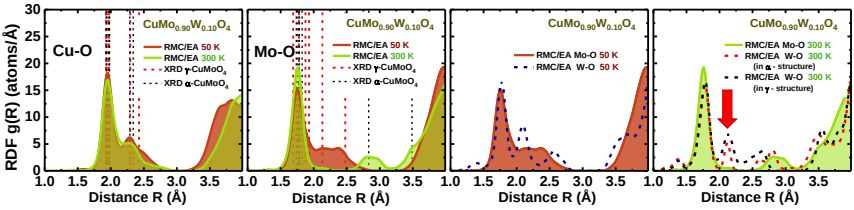

Figure 6.2.3: ***Radial distribution functions for Cu–O, Mo–O, W–O atom pairs in*** $\mathbf{CuMo_{0.90}W_{0.10}O_4}$*, calculated from the coordinates of the RMC/EA models. Dashed vertical lines show interatomic distances according to XRD data [1]. Red arrow indicates a group of oxygen atoms which does not exist in the tetrahedral coordination.*

These results confirm the tendency of tungsten atoms in α-$CuMo_{0.90}W_{0.10}O_4$ solid solutions to adapt more distorted environment that is closer to the octahedral than tetrahedral atomic configuration with oxygen atoms, thus affecting the temperature/pressure of α-to-γ phase transition and helping to stabilize γ-phase at room temperature.

6.3. RXES study at the W L_3-edge of $CuMo_{1-x}W_xO_4$ [4]

$CuMo_{1-x}W_xO_4$ solid solutions were studied by the resonant X-ray emission spectroscopy (RXES) study at the W L_3-edge to follow a variation of the tungsten local atomic and electronic structures across observed thermochromic phase transition as a function of sample composition and temperature. The experimental results were supplemented with *ab initio* calculations [28].

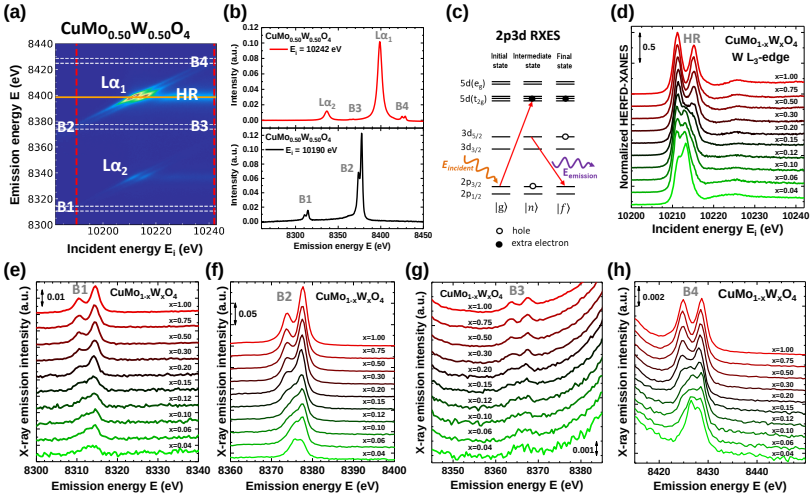

Figure 6.3.1: ***Composition-dependent RXES experimental data of $CuMo_{1-x}W_xO_4$ solid solutions:*** *RXES intensity map as a function of incident and emitted energies for $CuMo_{0.50}W_{0.50}O_4$ measured at 300 K (a). Vertical cuts of the RXES plane at the incident energies E_i=10190 eV and 10242 eV, shown in (a) by red dashed lines. Observed bands ($L\alpha_1$, α_2 and B1-B4) are labelled (b). A schematic diagram of 2p3d RXES process for an atom in octahedral coordination (c). The W L_3-edge HERFD-XANES spectra for different $CuMo_{1-x}W_xO_4$ solid solutions measured at the emission energy E_e=8398.5±0.2 eV, indicated by the horizontal orange line in (a) are shown in the panel (d). High energy resolution off-resonant X-ray emission spectra for different $CuMo_{1-x}W_xO_4$ solid solutions obtained with incident energy E_i=10190 eV – below the W L_3-edge (e,g) and at E_i=10242 eV – above the W L_3-edge (f,h).*

The analysis of the RXES plane (Fig. 6.3.1) provides valuable information on the coordination of tungsten atoms in the sample bulk and allows

[4] The main results, presented in this chapter, have been published as I. Pudza, A. Kalinko, A. Cintins, A. Kuzmin, **Study of the thermochromic phase transition in $CuMo_{1-x}W_xO_4$ solid solutions at the W L_3-edge by resonant X-ray emission spectroscopy**, Acta Mater. 205 (**2021**) 116581.

one to determine the crystal field splitting parameter Δ for the 5d(W)-states (Fig. 6.3.2). Moreover, this information can be extracted from the analysis of the RXES plane using different perspectives: the high energy resolution fluorescence detected X-ray absorption near-edge structure (HERFD-XANES) and the high energy resolution off-resonant X-ray emission spectra excited below and above resonance conditions (Fig.6.3.1). The analysis of RXES planes shows a clear advantage over conventional XANES due to revealing spectral features with much higher resolution.

It was found that tungsten ions in $CuMo_{1-x}W_xO_4$ solid solutions have octahedral coordination for samples with $x > 0.15$ both at low and high temperatures, whereas their coordination changes from tetrahedral to octahedral upon cooling down to 90 K for smaller W content (Fig. 6.3.2(a)). Nevertheless, at 300 K for solid solution with $x < 0.15$ some amount of tungsten ions co-exists in the octahedral environment. The obtained results correlate well with the optical properties of these materials, namely, colour change from greenish to brown upon cooling or increasing tungsten concentration.

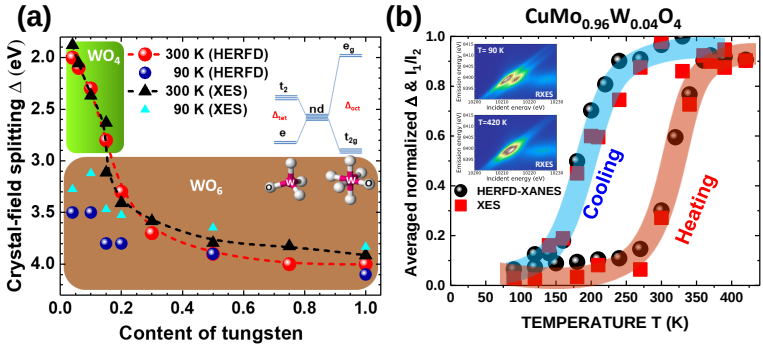

Figure 6.3.2: ***Crystal field splitting parameter Δ as a function of x in $CuMo_{1-x}W_xO_4$ at 90 K and 300 K****: calculated from off-resonant XES (Fig. 6.3.1(f)) and HERFD-XANES (Fig. 6.3.1(d)) spectra. A schematic energy level diagram showing crystal field splitting of 5d(W)-states in the tetrahedral and octahedral environment is also shown (a).* ***Temperature-dependent RXES data for $CuMo_{0.96}W_{0.04}O_4$****: Parts of the RXES planes at 90 K and 420 K on heating. Averaged value of normalized magnitude of the peak splitting (Δ) and the ratio of peak intensities (I_1/I_2) as a function of temperature (b).*

The RXES method is well suited for *in situ* measurements and was used here to track the hysteresis loop of the first-order structural phase transition between α and γ phases in $CuMo_{1-x}W_xO_4$ solid solutions on cooling and heating, even at low ($x < 0.10$) tungsten content (Fig. 6.3.2(b)). The spectral shape changes reflect the transitions between tetrahedral (α-phase) and octahedral (γ-phase) tungsten coordination.

6.4. XAS study of $Cu_{1-x}Zn_xMoO_4$ [5]

Here the influence of Zn^{2+} ions on the thermochromic properties of $Cu_{1-x}Zn_xMoO_4$ (x=0.10, 0.50, 0.90) solid solutions is shortly discussed.

The XANES and EXAFS spectra analysis revealed that the substitution of Cu^{2+} by Zn^{2+} ions stabilizes the α-phase, which is natural for α-$ZnMoO_4$. The substitution modifies the electronic structure of the solid solutions due to the presence of the Jahn-Teller effect for Cu^{2+} ions with $3d^9$ electronic configuration and absence of it for Zn^{2+} ions with filled 3d subshell.

Among sampled solid solutions, only $Cu_{0.90}Zn_{0.10}MoO_4$ exhibited thermochromic phase transition between α and γ phases with the hysteresis behaviour (Fig. 6.4.1). From the Mo K-edge XANES analysis, about 50% of the α-$Cu_{0.90}Zn_{0.10}MoO_4$ transforms to the low-temperature γ-phase at $T_{1/2C}$≈134 K during cooling, whereas 50% of the γ-$Cu_{0.90}Zn_{0.10}MoO_4$ transforms back to the α-phase at $T_{1/2H}$≈226 K upon heating. These temperatures are smaller than those for pure $CuMoO_4$.

A detailed analysis of the MSRD factors for metal-oxygen bonds within the first coordination shell was performed. We found that the substitution of copper by zinc affects the local environment of Mo^{6+} ions strongly. This result can be explained by the instability of molybdenum coordination, which is tetrahedral in α-$Cu_{0.90}Zn_{0.10}MoO_4$ solid solution but changes to distorted octahedral under lattice contraction at low temperatures in γ-$Cu_{0.90}Zn_{0.10}MoO_4$. This effect is similar to the temperature or pressure-induced α-to-γ phase transitions in $CuMoO_4$ [1]. Thus, tuning the thermochromic properties of $CuMoO_4$ by doping with zinc may find applications for monitoring storage conditions in the low-temperature range.

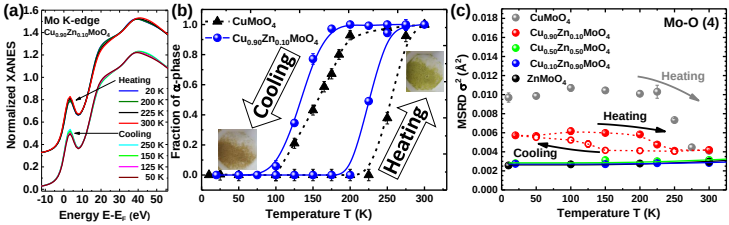

Figure 6.4.1: ***Temperature dependence of $Cu_{0.90}Zn_{0.10}MoO_4$****: experimental Mo K-edge XANES (a). Temperature dependence of the α-phase fraction in $CuMoO_4$ and $Cu_{0.90}Zn_{0.10}MoO_4$. Photographs of the $Cu_{0.90}Zn_{0.10}MoO_4$ sample at 77 K (brownish) and 300 K (green) are also shown (b). MSRD factors, obtained in RMC/EA simulations for the nearest 4 Mo–O atom pairs in $Cu_{1-x}Zn_xMoO_4$ (c).*

[5] The main results, presented in this chapter, have been published as I. Pudza, A. Anspoks, A. Cintins, A. Kalinko, E. Welter, A. Kuzmin, **The influence of Zn^{2+} ions on the local structure and thermochromic properties of $Cu_{1-x}Zn_xMoO_4$ solid solutions**, Materials Today Communications 28 (**2021**) 102607.

Summary and conclusions

In this thesis, the results of temperature and composition-dependent X-ray absorption and resonant X-ray emission spectroscopy (XAS and RXES) studies of copper molybdate ($CuMoO_4$) and its solid solutions with tungsten ($CuMo_{1-x}W_xO_4$) and zinc ($Cu_{1-x}Zn_xMoO_4$) are presented. High quality XAS and RXES experimental data were obtained during four experiments conducted at synchrotron radiation facilities.

The interpretation of EXAFS and XANES spectra is not straightforward and often requires advanced simulation tools, especially for such low symmetry materials as $CuMoO_4$ and related solid solutions. It was shown that while treatment of thermal fluctuations and static disorder in XAS is a complex task, it can be successfully addressed by RMC/EA simulations coupled with *ab initio* mutiple-scattering calculations. However, simple linear combination analysis of XANES data and the regularization-based method of EXAFS data analysis can also give valuable information on the local structure in the material.

Local structure probes allowed us to investigate the relationship between structural and thermochromic properties of $CuMoO_4$ in the temperature range between 10 and 973 K. EXAFS spectra analysis at several absorption edges simultaneously by the RMC/EA method allowed us to obtain 3D structure models of $CuMoO_4$ and its solid solutions and to analyse them in details.

The analysis of XAS data in the low-temperature range (10–300 K) allowed us to reconstruct the hysteresis of α-to-γ phase transition in $CuMoO_4$. Based on these data, the γ-to-α phase transition occurs in the temperature range of 230–280 K upon heating, whereas the α-to-γ transition occurs between 120 and 200 K upon cooling. During heating γ-$CuMoO_4$, molybdenum coordination by oxygen atoms gradually changes from strongly distorted octahedral to less distorted tetrahedral. At 250 K, the sample consisted of $\sim$60% γ-phase and $\sim$40% α-phase. The analysis of the Mo K-edge EXAFS spectra using the regularization-like method and RMC/EA simulations (simultaneously at the Mo and Cu K-edges) allowed us to obtain a temperature dependence of RDFs $g(R)$(Mo–O) and confirmed that the γ-to-α phase transition occurs gradually within a temperature range of 225–275 K. The influence of thermal effects on the local environment around molybdenum atoms in both γ and α phases is relatively weak, and the disorder is dominated by static distortions.

$CuMo_{0.90}W_{0.10}O_4$ solid solution exhibits thermochromic properties similar to pure $CuMoO_4$. The addition of 10 mol% of tungsten to $CuMoO_4$ induces local distortions and stabilizes the γ-phase, leading to an increase of the phase transition temperature by $\sim$50–100 K.

The XANES and EXAFS spectra analysis revealed that the substitution of Cu^{2+} ions by Zn^{2+} ions stabilizes the α-phase, which is natural for α-$ZnMoO_4$. The substitution modifies the electronic structure of the solid solutions due to the presence of the Jahn-Teller effect for Cu^{2+} ions with $3d^9$ electronic configuration and absence of it for Zn^{2+} ions with filled 3d subshell. In $Cu_{0.90}Zn_{0.10}MoO_4$, the phase transition hysteresis shifts to lower temperatures ($T_{1/2C}\approx$134 K and $T_{1/2H}\approx$226 K), while larger Zn^{2+} concentration stabilizes α-phase in all low-temperature range. The substitution of copper by zinc affects the local environment of Mo^{6+} ions strongly. This result can be explained by the instability of molybdenum coordination, which is tetrahedral in α-phase but changes to distorted octahedral under lattice contraction at low temperatures in γ-phase.

Tuning the thermochromic properties of $CuMoO_4$ to more desired temperature range by doping with tungsten or zinc may be the key for the material to find applications as an indicator for monitoring storage/processing conditions of temperature-sensitive products.

The thermochromic properties of $CuMoO_4$ in the high-temperature range (300–973 K) are not related to any phase transition. It was found that the local environment of copper atoms is more affected during heating than that of molybdenum atoms. It was shown that thermal disorder affects strongly not only the Cu K-edge EXAFS but also XANES region.

The RMC/EA simulations allowed us to obtain 3D structure models of $CuMoO_4$ as a function of temperature taking into account the thermal disorder effect. At the same time, they are able to reproduce the average positions (the Wyckoff positions) of atoms inside the unit cell in agreement with known diffraction data. The structural models obtained by the RMC/EA simulations were used to calculate the configuration-averaged Cu K-edge XANES using *ab initio* full-multiple-scattering theory. The calculated XANES spectra agree with the experimental data and qualitatively reproduce the main temperature-dependent XANES features. While the MoO_4 tetrahedra behave mostly as the rigid units, a reduction of the correlation in atomic motion between copper and axial oxygen atoms occurs upon temperature increase. This dynamic effect is the main cause of the temperature-induced changes in the $O^{2-}\rightarrow Cu^{2+}$ charge transfer processes and, thus, affects the thermochromic properties of α-$CuMoO_4$ upon heating above room temperature.

A variation of the EXAFS spectra at the metal absorption edges in $CuMo_{1-x}W_xO_4$ strongly correlates with Mo:W ratio. It was shown that multiple-scattering effects play an important role in the analysis of $CuMo_{1-x}W_xO_4$ solid solutions and should be taken into account to describe the contributions from the outer coordination shells accurately. At room temperature, $CuMo_{1-x}W_xO_4$ solid solutions with tungsten content above $x\sim$0.15 have the wolframite-type $CuMoO_4$-III phase isostructural to $CuWO_4$.

The ability of molybdenum atoms to adopt a locally distorted environment allows them to adjust to the solid solution structure determined by tungsten-related sublattice.

The role of tungsten ions was studied in more detail using RXES at the W L_3-edge (2p3d RXES), which allowed us to trace the crystal field induced splitting of the 5d states of tungsten. Moreover, this information can be extracted from the analysis of RXES plane using different approaches: the high-energy resolution fluorescence detected X-ray absorption near-edge structure (HERFD-XANES) and the high energy resolution off-resonant X-ray emission spectra excited below and above resonance conditions. The analysis of the experimentally obtained RXES planes shows a clear advantage over conventional XANES due to revealing spectral features with much higher resolution.

It was found that tungsten ions in $CuMo_{1-x}W_xO_4$ solid solutions always have octahedral coordination for samples with $x > 0.15$, whereas their coordination changes from tetrahedral to octahedral upon cooling for smaller tungsten content. Nevertheless, some amount of tungsten ions co-exists in the octahedral environment at 300 K for solid solutions with $x < 0.15$. The obtained results correlate well with the thermochromic properties of these materials, namely, colour change from greenish to brown upon cooling or increasing tungsten concentration.

The electronic structure of $CuMo_{1-x}W_xO_4$ solid solutions governs their thermochromic properties, which are related to the variation of the transmission window in optical spectra [6,7]. A change in the tungsten local coordination from tetrahedral to octahedral affects the band gap, which is determined by the oxygen-to-metal charge transfer [6]. The band gap is smaller in the case of octahedral coordination of tungsten [7], i.e., in solid solutions with higher tungsten content or lower temperature.

Main conclusions:

- XAS and RXES techniques are well suited for local structure studies in low-symmetry materials such as $CuMoO_4$ and its solid solutions.
- Thermal disorder in $CuMoO_4$ at high temperatures affects stronger the local environment of copper atoms than that of molybdenum.
- The thermochromic phase transition of $CuMoO_4$ at low temperatures is related to the change of molybdenum coordination between distorted octahedral and tetrahedral.
- An addition of tungsten and zinc ions to $CuMoO_4$ modifies its thermochromic properties.

Main theses

1. The hysteresis of the thermochromic phase transition between α and γ phases in $CuMoO_4$, occurring in the temperature range of 120–280 K and related to the gradual transformation of strongly distorted octahedral molybdenum coordination by oxygen atoms to less distorted tetrahedral, can be successfully probed by X-ray absorption spectroscopy at the Mo K-edge.
   *(Published in **[A6, A7]**.)*

2. In pure $CuMoO_4$ at temperatures above 300 K, the local environment of Cu atoms is more affected by the thermal disorder than that of Mo atoms. While the MoO_4 tetrahedra behave mostly as rigid units, a reduction of the correlation in atomic motion between copper and axial oxygen atoms occurs upon heating. This dynamic effect is the main cause of the temperature-induced changes in the $O^{2-} \rightarrow Cu^{2+}$ charge transfer processes and, thus, is the origin of the thermochromic properties of α-$CuMoO_4$.
   *(Published in **[A5]**.)*

3. *In situ* high energy resolution fluorescence detected X-ray absorption near-edge structure (HERFD-XANES) and the high energy resolution off-resonant X-ray emission spectra excited below and above resonance conditions at the W L_3-edge allow one to obtain the crystal field splitting parameter for the 5d(W)-states and, thus, to follow the coordination of tungsten atoms in $CuMo_{1-x}W_xO_4$ solid solutions.
   *(Published in **[A2]**.)*

4. In $CuMo_{1-x}W_xO_4$ ($x \leq 0.10$) solid solutions, the addition of W^{6+} ions induces local structural distortions and stabilizes γ-phase that leads to a shift of the phase transition hysteresis to higher temperatures. The addition of Zn^{2+} ions, in turn, stabilizes α-phase and shifts the phase transition hysteresis of $Cu_{1-x}Zn_xMoO_4$ ($x \leq 0.10$) to lower temperatures. Both W^{6+} and Zn^{2+} ion additions thus modify the thermochromic behaviour of the material.
   *(Published in **[A1, A3]**.)*

Bibliography

[1] M. Wiesmann, H. Ehrenberg, G. Miehe, T. Peun, H. Weitzel, and H. Fuess, "$p - T$ phase diagram of $CuMoO_4$," *J. Solid State Chem.*, vol. 132, pp. 88–97, 1997.

[2] M. Gaudon, P. Deniard, A. Demourgues, A. E. Thiry, C. Carbonera, A. Le Nestour, A. Largeteau, J. F. Létard, and S. Jobic, "Unprecedented "one-finger-push"-induced phase transition with a drastic color change in an inorganic material," *Adv. Mater.*, vol. 19, pp. 3517–3519, 2007.

[3] M. Gaudon, C. Riml, A. Turpain, C. Labrugere, and M. H. Delville, "Investigation of the chromic phase transition of $CuMo_{0.9}W_{0.1}O_4$ induced by surface protonation," *Chem. Mater.*, vol. 22, pp. 5905–5911, 2010.

[4] L. Robertson, N. Penin, V. Blanco-Gutierrez, D. Sheptyakov, A. Demourgues, and M. Gaudon, "$CuMo_{0.9}W_{0.1}O_4$ phase transition with thermochromic, piezochromic, and thermosalient effects," *Journal of Materials Chemistry C*, vol. 3, pp. 2918–2924, 2015.

[5] N. Joseph, J. Varghese, M. Teirikangas, and H. Jantunen, "A temperature-responsive copper molybdate polymorph mixture near to water boiling point by a simple cryogenic quenching route," *ACS Appl. Mater. Interfaces*, vol. 12, pp. 1046–1053, 2020.

[6] M. Gaudon, C. Carbonera, A. E. Thiry, A. Demourgues, P. Deniard, C. Payen, J. F. Létard, and S. Jobic, "Adaptable thermochromism in the $CuMo_{1-x}W_xO_4$ series ($0 \leq x < 0.1$): A behavior related to a first-order phase transition with a transition temperature depending on x," *Inorg. Chem.*, vol. 46, pp. 10 200–10 207, 2007.

[7] X. Wu, C. Fu, J. Cao, C. Gu, and W. Liu, "Effect of W doping on phase transition behavior and dielectric relaxation of $CuMoO_4$ obtained by a modified sol-gel method," *Mater. Res. Express*, vol. 7, p. 016309, 2020.

[8] A. Seeboth and D. Lötzsch, *Thermochromic and thermotropic materials*. CRC Press, 2013.

[9] G. Steiner, R. Salzer, and W. Reichelt, "Temperature dependence of the optical properties of $CuMoO_4$," *Fresenius J. Anal. Chem.*, vol. 370, pp. 731–734, 2001.

[10] J. Timoshenko, A. Kuzmin, and J. Purans, "EXAFS study of hydrogen intercalation into ReO_3 using the evolutionary algorithm," *Journal of Physics: Condensed Matter*, vol. 26, p. 055401, 2014.

[11] Y. Joly, "X-ray absorption near-edge structure calculations beyond the muffin-tin approximation," *Physical Review B*, vol. 63, p. 125120, 2001.

[12] O. Bunău and Y. Joly, "Self-consistent aspects of x-ray absorption calculations," *Journal of Physics: Condensed Matter*, vol. 21, p. 345501, 2009.

[13] A. Kuzmin, "Application of cluster computing in materials science," *Latvian Journal of Physics and Technical Sciences*, pp. 7–14, 2006.

[14] M. Newville, "Fundamentals of XAFS," *Reviews in Mineralogy and Geochemistry*, vol. 78, pp. 33–74, 2014.

[15] J. J. Rehr and R. C. Albers, "Theoretical approaches to x-ray absorption fine structure," *Reviews of modern physics*, vol. 72, p. 621, 2000.

[16] J. Timoshenko and B. Roldan Cuenya, "In Situ/Operando Electrocatalyst Characterization by X-ray Absorption Spectroscopy," *Chemical Reviews*, vol. 121, pp. 882–961, 2020.

[17] A. Kuzmin, "EDA: EXAFS data analysis software package," *Physica B: Condensed Matter*, vol. 208, pp. 175–176, 1995.

[18] J. D. Gale and A. L. Rohl, "The general utility lattice program (GULP)," *Mol. Simul.*, vol. 29, p. 291, 2003.

[19] S. Plimpton, "Fast parallel algorithms for short-range molecular dynamics," *Journal of computational physics*, vol. 117, pp. 1–19, 1995.

[20] N. Metropolis, A. W. Rosenbluth, M. N. Rosenbluth, A. H. Teller, and E. Teller, "Equation of state calculations by fast computing machines," *Journal of Chemical Physics*, vol. 21, pp. 1087–1092, 1953.

[21] R. McGreevy and L. Pusztai, "Reverse Monte Carlo simulation: a new technique for the determination of disordered structures," *Molecular simulation*, vol. 1, pp. 359–367, 1988.

[22] J. Timoshenko, A. Kuzmin, and J. Purans, "Reverse Monte Carlo modeling of thermal disorder in crystalline materials from EXAFS spectra," *Computer Physics Communications*, vol. 183, pp. 1237–1245, 2012.

[23] J. Timoshenko and A. Kuzmin, "Wavelet data analysis of EXAFS spectra," *Computer Physics Communications*, vol. 180, pp. 920–925, 2009.

[24] F. De Groot and A. Kotani, *Core level spectroscopy of solids*. CRC press, 2008.

[25] P. Glatzel and U. Bergmann, "High resolution 1s core hole X-ray spectroscopy in 3d transition metal complexes—electronic and structural information," *Coordination chemistry reviews*, vol. 249, pp. 65–95, 2005.

[26] P. Glatzel, M. Sikora, G. Smolentsev, and M. Fernández-García, "Hard X-ray photon-in photon-out spectroscopy," *Catalysis Today*, vol. 145, pp. 294–299, 2009.

[27] W. Błachucki, J. Hoszowska, J.-C. Dousse, Y. Kayser, R. Stachura, K. Tyrała, K. Wojtaszek, J. Sá, and J. Szlachetko, "High energy resolution off-resonant spectroscopy: A review," *Spectrochimica Acta B*, vol. 136, pp. 23–33, 2017.

[28] I. Pudza, A. Kalinko, A. Cintins, and A. Kuzmin, "Study of the thermochromic phase transition in $CuMo_{1-x}W_xO_4$ solid solutions at the W L_3-edge by resonant X-ray emission spectroscopy," *Acta Materialia*, vol. 205, p. 116581, 2021.

[29] F. Rodríguez, D. Hernández, J. Garcia-Jaca, H. Ehrenberg, and H. Weitzel, "Optical study of the piezochromic transition in $CuMoO_4$ by pressure spectroscopy," *Phys. Rev. B*, vol. 61, pp. 16 497–16 501, 2000.

[30] H. Ehrenberg, H. Weitzel, H. Paulus, M. Wiesmann, G. Wltschek, M. Geselle, and H. Fuess, "Crystal structure and magnetic properties of $CuMoO_4$ at low temperature (γ-phase)," *J. Phys. Chem. Solids*, vol. 58, pp. 153–160, 1997.

[31] T. Ito, H. Takagi, and T. Asano, "Drastic and sharp change in color, shape, and magnetism in transition of $CuMoO_4$ single crystals," *Chem. Mater.*, vol. 21, pp. 3376–3379, 2009.

[32] A.-E. Thiry, M. Gaudon, C. Payen, N. Daro, J.-F. Létard, S. Gorsse, P. Deniard, X. Rocquefelte, A. Demourgues, M.-H. Whangbo, and S. Jobic, "On the Cyclability of the Thermochromism in $CuMoO_4$ and Its Tungsten Derivatives $CuMo_{1-x}W_xO_4$ (x <0.12)," *Chem. Mater.*, vol. 20, p. 2075, 2008.

[33] S. C. Abrahams, J. L. Bernstein, and P. B. Jamieson, "Crystal structure of the transition-metal molybdates and tungstates. IV. Paramagnetic $CuMoO_4$," *J. Chem. Phys.*, vol. 48, pp. 2619–2629, 1968.

[34] D. Hernández, F. Rodrıguez, J. Garcia-Jaca, H. Ehrenberg, and H. Weitzel, "Pressure-dependence on the absorption spectrum of $CuMoO_4$: study of the green→ brownish-red piezochromic phase transition at 2.5 kbar," *Physica B: Condensed Matter*, vol. 265, pp. 181–185, 1999.

[35] S. Dey, R. A. Ricciardo, H. L. Cuthbert, and P. M. Woodward, "Metal-to-metal charge transfer in AWO_4 (A = Mg, Mn, Co, Ni, Cu, or Zn) compounds with the wolframite structure," *Inorg. Chem.*, vol. 53, p. 4394, 2014.

[36] I. Yanase, T. Mizuno, and H. Kobayashi, "Structural phase transition and thermochromic behavior of synthesized W-substituted $CuMoO_4$," *Ceramics International*, vol. 39, pp. 2059–2064, 2013.

[37] M. Benchikhi, R. El Ouatib, S. Guillemet-Fritsch, L. Er-Rakho, and B. Durand, "Investigation of structural transition in molybdates $CuMo_{1-x}W_xO_4$ prepared by polymeric precursor method," *Processing and Application of Ceramics*, vol. 11, pp. 21–26, 2017.

[38] W. Reichelt, T. Weber, T. Söhnel, and S. Däbritz, "Mischkristallbildung im System $CuMoO_4/ZnMoO_4$," *Zeitschrift für anorganische und allgemeine Chemie*, vol. 626, pp. 2020–2027, 2000.

[39] U. Steiner, W. Reichelt, and S. Däbritz, "Chemischer Transport von Mischkristallen im System $CuMoO_4/ZnMoO_4$," *Zeitschrift für anorganische und allgemeine Chemie*, vol. 629, pp. 116–122, 2003.

[40] A. Sleight and B. Chamberland, "Transition metal molybdates of the type $AMoO_4$," *Inorganic Chemistry*, vol. 7, pp. 1672–1675, 1968.

[41] T. Asano, T. Nishimura, S. Ichimura, Y. Inagaki, T. Kawae, T. Fukui, Y. Narumi, K. Kindo, T. Ito, S. Haravifard *et al.*, "Magnetic ordering and tunable structural phase transition in the chromic compound $CuMoO_4$," *Journal of the Physical Society of Japan*, vol. 80, p. 093708, 2011.

[42] I. Yanase, R. Koda, R. Kondo, and R. Taiji, "Improvement of thermochromic property at low temperatures of $CuMo_{0.94}W_{0.06}O_4$ by Zn substitution," *Journal of Thermal Analysis and Calorimetry*, pp. 1–12, 2019.

[43] S. K. Tiwari, A. Singh, P. Yadav, B. K. Sonu, R. Verma, S. Rout, and E. Sinha, "Structural and dielectric properties of Cu-doped α-$ZnMoO_4$ ceramic system for enhanced green light emission and potential microwave applications," *Journal of Materials Science: Materials in Electronics*, pp. 1–9, 2020.

[44] L. Cornu, V. Jubera, A. Demourgues, G. Salek, and M. Gaudon, "Luminescence properties and pigment properties of A-doped (Zn, Mg) MoO_4 triclinic oxides (with A= Co, Ni, Cu or Mn)," *Ceramics International*, vol. 43, pp. 13 377–13 387, 2017.

[45] E. Welter, R. Chernikov, M. Herrmann, and R. Nemausat, "A beamline for bulk sample x-ray absorption spectroscopy at the high brilliance storage ring PETRA III," in *AIP Conference Proceedings*, vol. 2054. AIP Publishing LLC, 2019, p. 040002.

[46] A. Di Cicco, G. Aquilanti, M. Minicucci, E. Principi, N. Novello, A. Cognigni, and L. Olivi, "Novel XAFS capabilities at ELETTRA synchrotron light source," in *J. Phys.: Conf. Ser.*, vol. 190, 2009, p. 012043.

[47] W. A. Caliebe, V. Murzin, A. Kalinko, and M. Görlitz, "High-flux XAFS-beamline P64 at PETRA III," *AIP Conf. Proc.*, vol. 2054, p. 060031, 2019.

[48] I. Jonane, A. Anspoks, G. Aquilanti, and A. Kuzmin, "High-temperature X-ray absorption spectroscopy study of thermochromic copper molybdate," *Acta Materialia*, vol. 179, pp. 26–35, 2019.

[49] I. Jonane, A. Cintins, A. Kalinko, R. Chernikov, and A. Kuzmin, "Low temperature X-ray absorption spectroscopy study of $CuMoO_4$ and $CuMo_{0.90}W_{0.10}O_4$ using reverse Monte-Carlo method," *Radiation Physics and Chemistry*, vol. 175, p. 108411, 2020.

[50] I. Pudza, A. Anspoks, A. Cintins, A. Kalinko, E. Welter, and A. Kuzmin, "The influence of Zn^{2+} ions on the local structure and thermochromic properties of $Cu_{1-x}Zn_xMoO_4$ solid solutions," *Materials Today Communications*, p. 102607, 2021.

[51] A. Kuzmin and J. Chaboy, "EXAFS and XANES analysis of oxides at the nanoscale," *IUCrJ*, vol. 1, pp. 571–589, 2014.

[52] B. Ravel and M. Newville, "ATHENA, ARTEMIS, HEPHAESTUS: data analysis for X-ray absorption spectroscopy using IFEFFIT," *J. Synchrotron Radiat.*, vol. 12, pp. 537–541, 2005.

[53] I. Jonane, A. Cintins, A. Kalinko, R. Chernikov, and A. Kuzmin, "Probing the thermochromic phase transition in $CuMoO_4$ by EXAFS spectroscopy," *Physica Status Solidi (B)*, vol. 255, p. 1800074, 2018.

[54] K.-i. Shimizu, H. Maeshima, H. Yoshida, A. Satsuma, and T. Hattori, "Ligand field effect on the chemical shift in XANES spectra of Cu(II) compounds," *Phys. Chem. Chem. Phys.*, vol. 3, pp. 862–866, 2001.

Author's publications

Publications directly related to the dissertation

A1. **I. Pudza**, A. Anspoks, A. Cintins, A. Kalinko, E. Welter, A. Kuzmin, The influence of Zn^{2+} ions on the local structure and thermochromic properties of $Cu_{1-x}Zn_xMoO_4$ solid solutions, *Mater. Today Commun.* 28 (**2021**) 102607, DOI:10.1016/j.mtcomm.2021.102607.

A2. **I. Pudza**, A. Kalinko, A. Cintins, A. Kuzmin, Study of the thermochromic phase transition in $CuMo_{1-x}W_xO_4$ solid solutions at the W L_3-edge by resonant X-ray emission spectroscopy, *Acta Mater.* 205 (**2021**) 116581, DOI:10.1016/j.actamat.2020.116581.

A3. **I. Jonane**, A. Cintins, A. Kalinko, R. Chernikov, A. Kuzmin, Low temperature X-ray absorption spectroscopy study of $CuMoO_4$ and $CuMo_{0.90}W_{0.10}O_4$ using reverse Monte-Carlo method, *Rad. Phys. Chem.* 175 (**2020**) 108112, DOI: 10.1016/j.radphyschem.2019.108411.

A4. A. Kuzmin, J. Timoshenko, A. Kalinko, **I. Jonane**, A. Anspoks, Treatment of disorder effects in X-ray absorption spectra beyond the conventional approach, *Rad. Phys. Chem.* 175 (**2020**) 108072, DOI: 10.1016/j.radphyschem.2018.12.032.

A5. **I. Jonane**, A. Anspoks, G. Aquilanti, A. Kuzmin, High-temperature X-ray absorption spectroscopy study of thermochromic copper molybdate, *Acta Mater.* 179 (**2019**) 26-35, DOI: 10.1016/j.actamat.2019.06.034.

A6. **I. Jonane**, A. Cintins, A. Kalinko, R. Chernikov, A. Kuzmin, Probing the thermochromic phase transition in $CuMoO_4$ by EXAFS spectroscopy, *Phys. Status Solidi B* 255 (**2018**) 1800074:1-5, DOI: 10.1002/pssb.201800074.

A7. **I. Jonane**, A. Cintins, A. Kalinko, R. Chernikov, A. Kuzmin, X-ray absorption near edge spectroscopy of thermochromic phase transition in $CuMoO_4$, *Low Temp. Phys.* 44 (**2018**) 568-572, DOI: 10.1063/1.5034155.

A8. **I. Jonane**, A. Kuzmin, and A. Anspoks, Advanced approach to the local structure reconstruction and theory validation on the example of the W L_3-edge extended X-ray absorption fine structure of tungsten, *Modelling Simul. Mater. Sci. Eng.* 26 (**2018**) 025004, DOI: 10.1088/1361-651X/aa9bab.

Other publications

B1. D. Bocharov, A. Chesnokov, G. Chikvaidze, J. Gabrusenoks, R. Ignatans, R. Kalendarev, M. Krack, K. Kundzins, A. Kuzmin, N. Mironova-Ulmane, **I. Pudza**, L. Puust, I. Sildos, E. Vasil'chenko, M. Zubkins, J. Purans, A comprehensive study of structure and properties of nanocrystalline zinc peroxide, *J. Phys. Chem. Solids* 160 (**2022**) 110318, DOI: 10.1016/j.jpcs.2021.110318.

B2. D. Bocharov, **I. Pudza**, K. Klementiev, M. Krack, A. Kuzmin, Study of high-temperature behaviour of ZnO by ab initio molecular dynamics simulations and X-ray absorption spectroscopy, *Materials* 14 (**2021**) 5206. DOI: 10.3390/ma14185206.

B3. J. Purans, A. P. Menushenkov, S. P. Besedin, A. A. Ivanov, V. S. Minkov, **I. Pudza**, A. Kuzmin, K. V. Klementiev, S. Pascarelli, O. Mathon, A. D. Rosa, T. Irifune, M. I. Eremets, Local electronic structure rearrangements and strong anharmonicity in YH_3 under pressures up to 180 GPa, *Nat. Commun.* 12 (**2021**) 1765, DOI: 10.1038/s41467-021-21991-x.

B4. F. C. Correia, J. M. Ribeiro, A. Kuzmin, **I. Pudza**, A. Kalinko, E. Welter, A. Mendes, J. Rodrigues, N. Ben Sedrine, T. Monteiro, M. R. Correia, C. J. Tavares, The role of Ga and Bi

doping on the local structure of transparent zinc oxide thin films, *J. Alloys Compd.* 870 (**2021**) 159489, DOI:10.1016/j.jallcom.2021.159489.

B5. B. Polyakov, E. Butanovs, A. Ogurcovs, S. Vlassov, M. Zubkins, **I. Jonane**, A. Cintins, A. Kalinko, A. Kuzmin, J. Purans, Understanding the conversion process of magnetron-deposited thin films of amorphous ReO_x to crystalline ReO_3 upon thermal annealing, *Cryst. Growth Des.* 20 (**2020**) 6147-6156, DOI:10.1021/acs.cgd.0c00848.

B6. J.M. Ribeiro, F.C. Correia, A. Kuzmin, **I. Jonane**, M. Kong, A.R. Goni, J.S. Reparaz, A. Kalinko, E. Welter, C.J. Tavares, Influence of Nb-doping on the local structure and thermoelectric properties of transparent TiO_2:Nb thin films, *J. Alloys Compd.* 838 (**2020**) 155561, DOI:10.1016/j.jallcom.2020.155561.

B7. L. Nataf, F. Baudelet, A. Polian, **I. Jonane**, A. Anspoks, A. Kuzmin, T. Irifune, Recent progress in high-pressure X-ray absorption spectroscopy studies at the ODE beamline, *High Pressure Res.* 40 (**2020**) 82-87, DOI: 10.1080/08957959.2019.1700979.

B8. T. Schenk, A. Anspoks, **I. Jonane**, R. Ignatans, B.S. Johnson, J.L. Jones, M. Tallarida, C. Marini, L. Simonelli, P. Hönicke, C. Richter, T. Mikolajick, U. Schroeder, Local structural investigation of hafnia-zirconia polymorphs in powders and thin films by X-ray absorption spectroscopy, *Acta Mater.* 180 (**2019**) 158-169, DOI:10.1016/j.actamat.2019.09.003.

B9. **I. Jonane**, A. Anspoks, L. Nataf, F. Baudelet, T. Irifune, A. Kuzmin, Pressure-induced structural changes in α-MoO_3 probed by X-ray absorption spectroscopy, *IOP Conf. Ser.: Mater. Sci. Eng.* 503 (**2019**) 012018, DOI: 10.1088/1757-899X/503/1/012018.

B10. **I. Jonane**, J.Timoshenko, and A. Kuzmin, Atomistic simulations of the Fe K-edge EXAFS in FeF_3 using molecular dynamics and reverse Monte Carlo methods, *Phys. Scr.* 91 (**2016**) 104001, DOI: 10.1088/0031-8949/91/10/104001.

B11. **I. Jonane**, K. Lazdins, J. Timoshenko, A. Kuzmin, J. Purans, P. Vladimirov, T. Gräning, J. Hoffmann, Temperature-dependent EXAFS study of the local structure and lattice dynamics in cubic Y_2O_3, *J. Synchrotron Rad.* (**2016**) 510-518, DOI: 10.1107/S1600577516001181.

B12. **I. Jonane**, J. Timoshenko, A. Kuzmin, EXAFS study of the local structure of crystalline and nanocrystalline Y_2O_3 using evolutionary algorithm method, *IOP Conf. Ser.: Mater. Sci. Eng.* 77 (**2015**) 012030:1-5, DOI: 10.1088/1757-899X/77/1/012030.

B13. J. Timoshenko, A. Anspoks, A. Kalinko, **I. Jonane**, A. Kuzmin, Local structure of multiferroic $MnWO_4$ and $Mn_{0.7}Co_{0.3}WO_4$ revealed by the evolutionary algorithm, *Ferroelectrics* 483 (**2015**) 68-74, DOI: 0.1080/00150193.2015.1058687.

Participation in international conferences and workshops

1. 14.08.-22.08.2021. – 25th Congress of International Union of Crystallography IUCr25
   oral presentation "*Treatment of disorder effects in X-ray absorption spectra by reverse Monte Carlo simulations: $CuMoO_4$ case*" (I. Pudza, A. Kuzmin).
2. 12.07.-13.07.2021. – International Conference on X-Ray Absorption Fine Structure - XAFS 2021 Virtual (online),
   oral presentation "*XAS and RXES studies of phase transitions in $CuMo_{1-x}W_xO_4$ solid solutions*" (I. Pudza, A. Kalinko, A. Cintins, A. Kuzmin).
3. 05.07.-07.07.2021. – YOUNG MULTIS - Multiscale Phenomena in Condensed Matter Online conference for young researchers (online),
   oral presentation "*Local structure studies of multifunctional $CuMoO_4$ and $CuWO_4$ solid solutions*" (I. Pudza, A. Kalinko, A. Cintins, A. Kuzmin).
4. 28.04.2021. – Bilateral workshop of Taiwan and the Baltic States Research Center on Physics (online),
   oral presentation "*Resonant X-ray emission spectroscopy to reveal coordination of W ions in $CuMo_{1-x}W_xO_4$ thermochromic materials*" (I. Pudza).

5. 25.01.-29.01.2021. – DESY Photon Science Users' Meeting 2021 (online),
   poster presentation "*Resonant X-ray emission spectroscopy of the thermochromic phase transition in $CuMo_{1-x}W_xO_4$ solid solutions*" (I. Pudza, A. Kalinko, A. Cintins, A. Kuzmin).
6. 22.01.2021. – DESY Photon Science Users' Meeting 2021 - Satellite meeting "X-Ray Absorption Spectroscopy at P64/65" (online),
   oral presentation "*Thermochromic phase transition in $CuMo_{1-x}W_xO_4$ solid solutions probed by Resonant X-ray emission spectroscopy at the W L_3-edge*" (I. Pudza, A. Kalinko, A. Cintins, A. Kuzmin).
7. 16.09.-20.09.2019. – EMRS Fall Meeting 2019 (Warsaw, Poland),
   poster presentation "*Temperature and doping induced evolution of the local structure of thermochromic copper molybdate*" (I. Jonane, A. Anspoks, A. Cintins, G. Aquilanti, A. Kalinko, R. Chernikov, A. Kuzmin).
8. 11.04.-12.04.2019. – 15th International Young Scientist conference "Developments in Optics and Communications 2018" (Riga, Latvia),
   poster presentation "*Structural investigations of $CuMo_{1-x}W_xO_4$ solid solution*" (I. Jonane, A. Cintins, A. Anspoks, G. Aquilanti, A. Kalinko, G. Aquilanti, A. Kuzmin).
9. 02.11.-05.11.2018. – 12th International Scientific Conference "Functional Materials and NanoTechnology" (Riga, Latvia),
   oral presentation "*Functional and structural properties of copper molybdate*" (I. Jonane, A. Anspoks, A. Cintins, G. Aquilanti, A. Kalinko, G. Aquilanti, R. Chernikov, A. Kuzmin) and
   poster presentation "*Pressure-induced structural changes in α-MoO_3 probed by X-ray absorption spectroscopy*" (I. Jonane, A. Anspoks, L. Nataf, F. Baudelet, T. Irifune, A. Kuzmin) - achieved poster prize.
10. 20.09.-22.09.2018. – conference "The First 30 Years of Reverse Monte Carlo Modelling" (Budapest, Hungary),
    oral presentation "*Treatment of disorder in XANES by RMC simulations*" (I. Jonane, A. Kuzmin).
11. 22.07.-27.07.2018. – 17th International Conference on X-Ray Absorption Fine Structure (Krakow, Poland),
    oral presentation "*Low temperature X-ray absorption spectroscopy study of $CuMoO_4$ and $CuMo_{0.90}W_{0.10}O_4$ using reverse Monte-Carlo method*" (I. Jonane, A. Cintins, A. Kalinko, R. Chernikov, A. Kuzmin).
12. 05.04.-06.04.2018. – 14th International Young Scientist conference "Developments in Optics and Communications 2018" (Riga, Latvia),
    oral presentation "*Structural investigations of thermochromic phase transition in copper molybdate*" (I. Jonane, A. Cintins, A. Kalinko, R. Chernikov, A. Kuzmin).
13. 12.03.-14.03.2018. – COST TO-BE (Towards oxide-based electronics (MP1308)) Spring Meeting (Sant Feliu de Guixols, Spain),
    poster presentation "*X-ray absorption spectroscopy for structural analysis of $CuMoO_4$*" (I. Jonane, A. Cintins, A. Anspoks, A. Kuzmin).
14. 11.09.-13.09.2017. – COST TO-BE (Towards oxide-based electronics (MP1308)) Fall Meeting (Riga, Latvia),
    poster presentation "*Temperature-dependent X-ray absorption spectroscopy study of $CuMoO_4$*" (I. Jonane, A. Kuzmin, A. Anspoks) - achieved poster prize.
15. 16.05.-19.05.2017. – 16. International conference of Plasma-Facing Materials and Components for Fusion Applications (Düsseldorf, Germany),
    poster presentation "*X-ray absorption spectroscopy study of yttria nanoparticles using simulation-based methods*" (I. Jonane, A. Kuzmin, A. Anspoks, A. Cintins, V.E. Serga, J. Purans) and
    poster presentation "*Advanced approach to the local structure reconstruction and theory validation on example of the W L_3-edge EXAFS of tungsten*" (I. Jonane, A. Kuzmin, A.

Anspoks).

16. 24.04.-27.04.2017. – 11th International Scientific Conference "Functional Materials and NanoTechnology" (Tartu, Estonia),
poster presentation "*Temperature-dependent EXAFS study of the local structure of copper molybdate using reverse Monte-Carlo method*" (I. Jonane, A. Kuzmin, A. Anspoks).
17. 06.04.-07.04.2017. – 13th International Young Scientist conference "Developments in Optics and Communications 2017" (Riga, Latvia),
oral presentation "*Relationship between local structure and optical properties of copper molybdate*" (I. Jonane, A. Anspoks, A. Kuzmin).
18. 10.06.-12.06.2015. – EURONANOFORUM 2015 (Riga, Latvia),
poster presentation "*Static disorder in nanocrystalline yttria probed by X-ray absorption spectroscopy*" (I. Jonane, J. Timoshenko, A. Kuzmin).
19. 08.04.-10.04.2015. – 11th International Young Scientist conference "Developments in Optics and Communications 2015" (Riga, Latvia),
oral presentation "*Temperature dependence of the local structure of Y_2O_3 from EXAFS analysis using evolutionary algorithm method*" (I. Jonane, J. Timoshenko, A. Kuzmin)
20. 29.09.-01.10.2014. – 9th International Scientific Conference "Functional Materials and NanoTechnology" (Riga, Latvia),
poster presentation "*EXAFS study of the local structure of crystalline and nanocrystalline Y_2O_3 using evolutionary algorithm method*" (I. Jonane, J. Timoshenko, A. Kuzmin).

Participation in international schools

1. 13.09.-17.09.2021. – 1st on-line School on Synchrotron Radiation "Gilberto Vlaic": Fundamentals, Methods and Application (online).
2. 05.11.-09.11.2019. – BESSY II visit within CALIPSOplus Twinning Programme - visit of HE-SGM beamline dedicated to NEXAFS/XPS spectroscopy experiments (Berlin, Germany).
3. 16.06.-21.06.2019. – ESRF synchrotron school "High-pressure techniques at the ESRF-EBS" (Grenoble, France), poster presentation "*High pressure effect on the local structure of α-MoO_3 and α-H_xMoO_3*".
4. 30.03.-05.04.2019. – MATRAC 2 School "Application of Neutrons and Synchrotron Radiation in Materials Science with special focus on Fundamental Aspects of Materials" (Munich, Germany), poster presentation "*Pressure-dependent X-ray absorption spectroscopy study of α-MoO_3 and α-H_xMoO_3*".
5. 15.03.-17.03.2018. – MP1308 COST TO-BE Action School "Technologies for oxide electronics" (Sant Feliu de Guixols, Spain).
6. 19.08.-26.08.2017. – RACIRI summer school "Grand Challenges and Opportunities with the Best X-ray and Neutron Sources" (Ronneby, Sweden), poster presentation "*Advanced analysis of X-ray absorption spectra: the case of tungsten*".
7. 01.03.-03.03.2017. – DESY research course "Nanoscience at Modern X-ray Sources" (Hamburg, Germany), poster presentation "*X-ray absorption spectroscopy study of nanocrystalline yttria*" - achieved poster prize.
8. 18.07.-22.07.2016. – 1st NFFA Europe Summer School "Nanoscience Foundries and Fine Analysis" (Barcelona, Spain), poster presentation "*RMC analysis of the Y K-edge EXAFS spectra in micro- and nano-crystalline Y_2O_3*".
9. 27.06.-06.07.2014. – Summer school at Merseburg Technical University "Basic Experiments in Sensor Technology and Laser Physics" (Merseburg, Germany).

Participation in synchrotron experiments[1]

1. 02.12.-06.12.2021. – XAS measurements within project "*X-ray absorption spectroscopy of medium-entropy alloys*" at PETRA III.
2. 26.11.-01.12.2021. – XAS measurements within project "*The colouration of tungstates by proton intercalation: the effect on the local structure*" at PETRA III.
3. 01.10.-04.10.2021. – XAS measurements within project "*Local structure instabilities and lattice dynamics in 2D layered materials upon charge-density-wave transitions*" at PETRA III.
4. 04.05.-10.05.2021. & 27.09-29.09.2021. – RXES measurements within project "*Temperature-dependent HERFD-XANES spectroscopy study of thermochromic effects in* $CuMo_{1-x}W_xO_4$ *at the Mo K-edge*" at PETRA III (remotely & on-site).
5. 29.10.-02.11.2020. – XAS measurements within project "*Local structure and disorder in thermoelectric ZnO:Sb thin films*" at PETRA III.
6. 29.09.-05.10.2020. – RXES measurements within project "*Resonant X-ray emission spectroscopy of polaronic effects in nanocrystalline tungstates*" at PETRA III.
7. 10.09.-14.09.2020. – XAS measurements within project "*Unravelling the structure of rhenium oxide thin films*" at PETRA III.
8. 25.11.-29.11.2019. – XAS measurements within project "***The influence of zinc ions on the thermochromic properties of*** $\boldsymbol{Cu_{1-x}Zn_xMoO_4}$ ***solid solutions***" at PETRA III.
9. 25.06.-01.07.2019. – XAS measurements within project "*Impact of pressure on the atomic structure and lattice dynamics in* ReS_2 *and* $ReSe_2$" at SOLEIL.
10. 23.05.-28.05.2019. – RXES measurements within project "***Resonant X-ray emission spectroscopy of mixed*** $\boldsymbol{CuMo_{1-x}W_xO_4}$ ***thermochromic materials***" at PETRA III.
11. 13.12.-17.12.2018. – XAS measurements within project "*X-ray absorption spectroscopy of oxide thermoelectric materials*" at PETRA III.
12. 13.05.-18.06.2018. – XAS measurements within project "*X-ray absorption spectroscopy of lattice dynamics in 2D layered materials*" at PETRA III.
13. 24.01.-29.01.2018. – XAS measurements within project "*Impact of pressure and electron doping on the lattice distortion in* α*-*MoO_3" at SOLEIL.
14. 22.06.-27.06.2017. – XAS measurements within project "*XAS Local Atomic Structure Studies of Ferroelectric* HfO_2" at PETRA III.
15. 03.11.-08.11.2016. – XAS measurements within project "***Low temperature thermochromic phase transition in*** $\boldsymbol{CuMo_{1-x}W_xO_4}$ ***solid solutions***" at PETRA III.
16. 26.05.-30.05.2016. – XAS measurements within project "*EXAFS study of negative thermal expansion in nanocrystalline CuO*" at PETRA III.
17. 07.12.-13.12.2015. – XAS measurements within project "***Study of the thermochromic phase transition in*** $\boldsymbol{CuMoO_4}$ ***and mixed*** $\boldsymbol{CuMo_{1-x}W_xO_4}$" at ELETTRA.

[1] PETRA III synchrotron is located in Hamburg, Germany, SOLEIL synchrotron – in Paris, France, ELETTRA synchrotron – in Trieste, Italy.

Acknowledgements

I want to express sincere gratitude to my supervisor Dr. phys. Alexei Kuzmin who helped, motivated and guided me during the whole period of my PhD studies. His immense knowledge, plentiful experience and continuous support have encouraged me in all the time of my research and daily life. I am genuinely grateful for the possibility to work under his leadership.

I would also like to express my special thanks to Dr. phys. Janis Timoshenko, who supported and inspired me during my first steps in science when I started work at the Institute during my Bachelor studies.

I would like to acknowledge my colleagues from the EXAFS spectroscopy laboratory - M.Sc. Arturs Cintins, Dr. phys. Andris Anspoks, Dr. rer. nat. Georgijs Bakradze - for the great working atmosphere they created in our laboratory and at synchrotron beamlines, conferences and schools all around Europe. A separate acknowledgement is expressed to Dr. phys. Aleksandr Kalinko for invaluable help and care during the experiments at PETRA III synchrotron.

And, of course, many thanks to my family for the patience and support throughout my studies. Special thanks to my husband Kaspars, mum Lolita and sister Laura. Thanks also to Ilze Oshina – my soulmate during the whole studies at the university.

I would like to thank the Institute of Solid State Physics for being a nice place where to work and develop my career. Additionally, I would like to acknowledge Scientific Research Projects for Students and Young Researchers No. SJZ/2017/5, No. SJZ/2018/1 and No. SJZ/2019/1 realized at the Institute of Solid State Physics, University of Latvia. Institute of Solid State Physics, University of Latvia as the Center of Excellence has received funding from the European Union's Horizon 2020 Framework Programme H2020-WIDESPREAD-01-2016-2017-TeamingPhase2 under grant agreement No. 739508, project CAMART2.

I also want to thank the Faculty of Physics, Mathematics and Optometry of the University of Latvia for the support during studies and research.

This research was financially supported by philanthropist MikroTik and administrated by the University of Latvia Foundation. This support was precious during my PhD studies.

Finally, I am deeply honoured for the prestigious prize in the year 2021 from the L'ORÉAL Baltic "For Women In Science" Program with the support of the Latvian National Commission for UNESCO and the Latvian Academy of Sciences.